UNITED NATIONS UNIVERSITY
UNU-GTP
Geothermal Training Programme

Orkustofnun, Grensasvegur 9,
IS-108 Reykjavik, Iceland

Reports 2017
Number 14

BOREHOLE GEOLOGY AND THERMAL HISTORY OF WELL OW-737, OLKARIA GEOTHERMAL FIELD, KENYA

Risper Jemutai Kandie
Kenya Electricity Generating Company, Ltd. – KenGen
P.O. Box 785
20117 Naivasha
KENYA
rkandie@kengen.co.ke, rkandie@gmail.com

ABSTRACT

OW-737 is a wildcat well drilled in the periphery of the Olkaria Northeast sub-sector of Olkaria geothermal field for the purpose of appraising the extent of the Olkaria geothermal system beyond the boundaries of the Northeast sub-sector. It is a vertical well drilled in 2016 to a total depth of 2998 m CT.

Lithostratigraphy established from the top to the bottom of the well comprises five lithological series, namely pyroclastics, rhyolites, basalts, trachytes and syenitic intrusions series with thin basaltic and rhyolitic dikes that occur within the trachytic series. Hydrothermal alteration minerals identified provide information on the paleotemperature of the geothermal reservoir as denoted by the presence of alteration minerals that represent low temperature (e.g. smectite, scolecite, mesolite), intermediate (e.g. quartz, chlorite) and high temperature (e.g. prehnite, epidote, wollastonite and actinolite) with increased depth. Five alteration mineral zones defined by the first appearance of alteration minerals are established: unaltered (0-208 m), zeolite-illite (208-604 m), chlorite-illite (604-856 m), epidote-chlorite-illite (856-1610 m) and actinolite-epidote-illite (1610-2990 m). This shows that high temperatures are indicated below 1000 m depth as defined by the epidote-chlorite-illite zone marking the top of the geothermal reservoir.

The paragenetic sequences of alteration minerals are categorized into alteration zones, indicating two temperature regimes where initially the temperature was high and later a cooling regime occurred, exemplified e.g. by calcite overprinting epidote at 1526 m depth. Calculated formation temperature, alteration mineral temperature and homogenization temperature (Th) from fluid inclusion analyses were compared. The results show great variation between formation and alteration temperatures, suggesting a cooling of the well. The homogenization temperature to some extent shows slight cooling in the well. Presence of minerals such as hematite at various horizons in the well could indicate the incursion of cooler fluids in the well. This seems to support the possibility of the well being located in a downflow zone, also considering its close proximity to the Gorge farm fault that is known to be the recharge conduit of the Olkaria geothermal reservoir. The injectivity of the well could not be determined as the well could not take in water during injection tests due to its current impermeability. Therefore, the permeability zones identified in relation to geological interpretations are presumably fossil.

1. INTRODUCTION

1.1 General Information

Olkaria geothermal field is the first, fully developed geothermal field in Kenya with a current installed capacity of 673.1 MWe. Geologically, it is located within the Kenya Rift, in the eastern branch of the East Africa Rift System (EARS), in which the geothermal prospects of Kenya occur, see Figure 1.

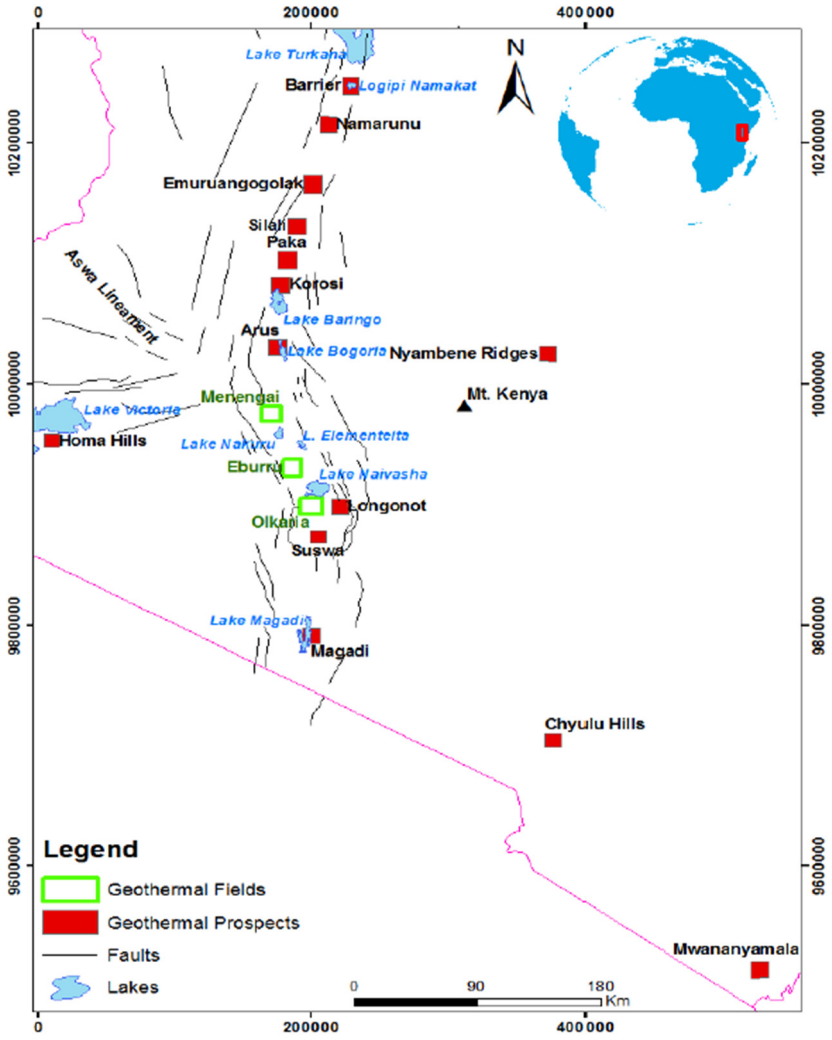

FIGURE 1: Map of the Kenya Rift showing the location of the Olkaria volcanic complex and other geothermal prospects (modified from Ofwona et al, 2006)

EARS is a divergent type of plate boundary situated above two mantle plumes: the Ethiopia Dome and Kenya Dome (Bosworth et al. 1998). Their formation was initiated with an extension that took place in the Red Sea and the Gulf of Aden about 30 Ma ago, when the African Plate (Nubian plate) rifted from the Arabian plate. The mantle plumes created a magmatic plumbing system that developed prior to continental rupture (Ebinger, 2005). Consequentially, they are responsible for morphological features of the rift system that include volcanic eruptions and crustal breakups such as horsts and grabens. The elevated mantle plume is responsible for the existence of convective heat flow in the lithospheric mantle at shallow depths, which influences tectonics and magmatism and hence the occurrence of several geothermal prospects. The East African Rift System is poorly dated but certainly preceded the graben development (Ring, 2014). The rifting in the EARS propagated south and separated into the Eastern and Western branches. The Kenya rift is located in the eastern branch, where it is centred on the hot spot represented by the Kenya domal uplift, which is elliptical in plan and about 1000 km wide. It has three rift arms, two of which form the main rift, whereas the third is subdued, trending west from the centre of the dome. The basins are controlled by faults and form subsiding grabens or troughs almost 100 km long, a few km wide and partially filled with sediments and/or volcanic rocks.

The Olkaria geothermal system is located in the Olkaria Volcanic Complex (OVC), which is situated in the central sector of the Kenya rift. In this part of the EARS, the crustal thickness is estimated to be 30-35 km (Mechie et al, 1997). Magmatism started in the late Pleistocene and has continued until recently as indicated by the Ololbutot comenditic lava flows dated at 180±50 years BP (Clarke et al., 1990). The

Olkaria Volcanic Complex is bordered by three geothermal prospects, namely Longonot, Eburru and Suswa to the east, north and south, respectively. Unlike the three prospects, the Olkaria volcanic complex lacks a distinct caldera and eruption centres. Simiyu and Keller (2000) postulated that a group of coalesced rhyolitic domes in the eastern and southern segments of the volcanic complex mark the rim of a caldera structure.

The Olkaria geothermal field is categorized as a high-enthalpy geothermal field with temperatures above 200°C at 1000 m depth. The approximate resource area under KenGen concession is 204 km^2. The field is divided into seven sub-fields for ease of characterization and development. The sub-fields are named East, Northeast, Central, Northwest, Domes, Southeast and Southwest fields, see Figure 2. Each field is at a different stage of development but exploitation and exploration studies for geothermal resources started back in the late 1950s. Since then, exploration, drilling and development has been ongoing. To date, close to 300 wells have been drilled across the fields, including production, injection, make-up and monitoring wells. Well depths range from 500 to 3650 m.

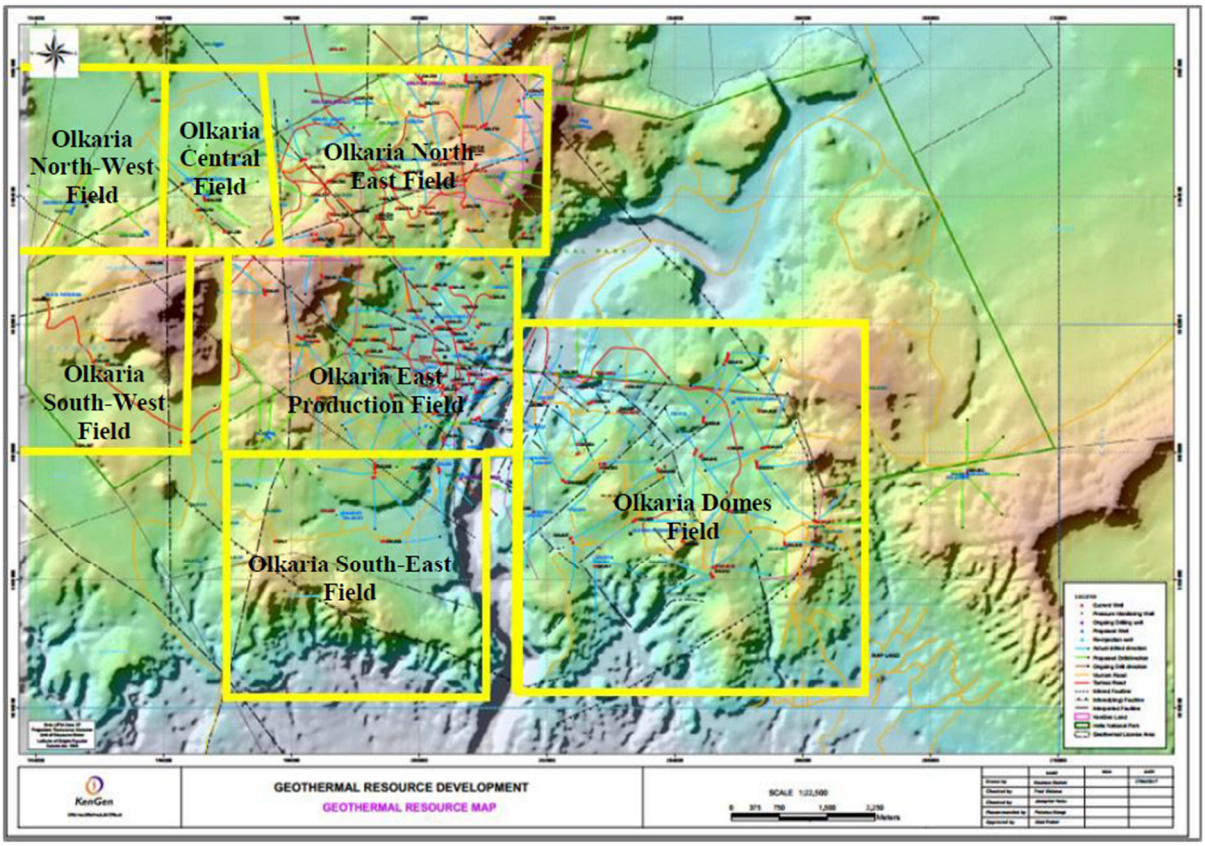

FIGURE 2: Map showing the sub sectors of the Olkaria geothermal field (modified from KenGen, 2017)

The current installed capacity of the Olkaria geothermal field is 683.1 MWe, which has been progressively developed with the installation of power plants of variable capacities at different times. Table 1 lists the existing power plants and the Olkaria V power plant (150 MWe) which is being constructed and is expected to be commissioned in 2019.

1.2 Overview of the Olkaria geothermal system

The Olkaria geothermal system has been under geoscientific assessment for a long time. With more data from geoscientific studies and drilling, the level of confidence to develop Olkaria has risen along with a better understanding of the geothermal resource. The conceptual model for Olkaria has therefore

TABLE 1: Electric energy generation from Olkaria power plants, their capacities and status (modified from Otieno, 2016)

Power plant	Year commissioned	No. of units	Status	Total installed capacity (MWe)	Total capacity (MWe)	Sub-sector
Olkaria 1	1981 (15 MWe) 1982 (15 MWe) 1985 (15 MWe)	3	Operating	45	45	East
Olkaria II	2003 (70 MWe) 2010 (35 MWe)	3	Operating	105	105	Northeast
Olkaria I (AU)	2015 (150 MWe)	2	Operating	150	140	East
Olkaria III (Orpower)	2000 (53 MWe) 2008 (39 MWe) 2014 (17 MWe) 2016 (30 MWe)	-	Operating	150	140	Southwest
Olkaria IV	2014 (150 MWe)	2	Operating	150	140	Domes
Olkaria Well Head Generation	2012-2017 (81.1 MWe)	15	Operating	81.1	81.1	Domes & East
Olkaria V		2	Construction	158		Domes

improved since Sweco and Virkir (1976) defined the Olkaria system as a boiling geothermal reservoir overlain by a steam zone, capped by tuffaceous cap rock. Ofwona (2002) postulated two possible up-flow zones in Olkaria Northeast and one up-flow zone in Olkaria East, with a down-flow in the two areas. This revision of the conceptual model further showed that extensive boiling also occurs in the up-flow zones to form steam caps below the cap rock. In the same model, cold water recharge into the Olkaria geothermal system is assumed to occur from all directions.

A West-JEC assessment in 2008-2009 found that the Olkaria geothermal system is considered to have a magma chamber, which has fed the most recent volcanic events in the area (West-JEC, 2009) It is furthermore believed to be a possibility that the magma chamber peaks in several locations, creating convective heat transfer above these and providing hot recharge to different parts of the geothermal system. In addition to up-flows in the Northeast and East sectors, such an up-flow is now proposed in the Domes sector as well. Further updates of the conceptual model were made by the Mannvit/ÍSOR/Vatnaskil/Verkís consortium (2012, 2015) which confirm that the Olkaria geothermal resource is capable of supporting a capacity of over 1000 MWe. Their report also confirms that the Olkaria geothermal system is sustained by hot upflow zones, which may be linked to deep-seated heat sources and are related to three main intrusions (Figure 3) possibly partially molten, extending up to 6-8 km depth from a deep-seated magma chamber proposed to lie beneath Olkaria Hill (Olkaria West), beneath the Gorge farm volcanic centre in the northeast, and in the Domes.

According to Saitet et al (2016), there are up to six upflow zones (temperature anomaly regions as denoted by red arrows in Figure 3) that are supported by the temperature model. They are in the East, Northeast, Domes, Southeast, West and below well OW-101. Furthermore, they concluded that the recharge (indicated by black arrows) to the system is sustained by the N-S trending Ololbutot fault and faults near well OW-501, with the ring structure also acting as a source for recharge all around the field and more so to the east.

1.3 Overview of Olkaria Northeast field

Olkaria Northeast field is one of the sub fields of the Greater Olkaria geothermal area (GOGA). It is a fully developed field with over 60 drilled wells that supply steam to the Olkaria II power plant (105 MWe) as well as geothermal fluid for the Olkaria Geothermal Spa. The potential of the geothermal resource on its periphery is under assessment. The wells drilled in the region have shown variable results. High producing wells have temperatures that are greater than 280°C, while poor producers have temperatures that are less than 150°C. Variations in the temperature characteristics of the wells are

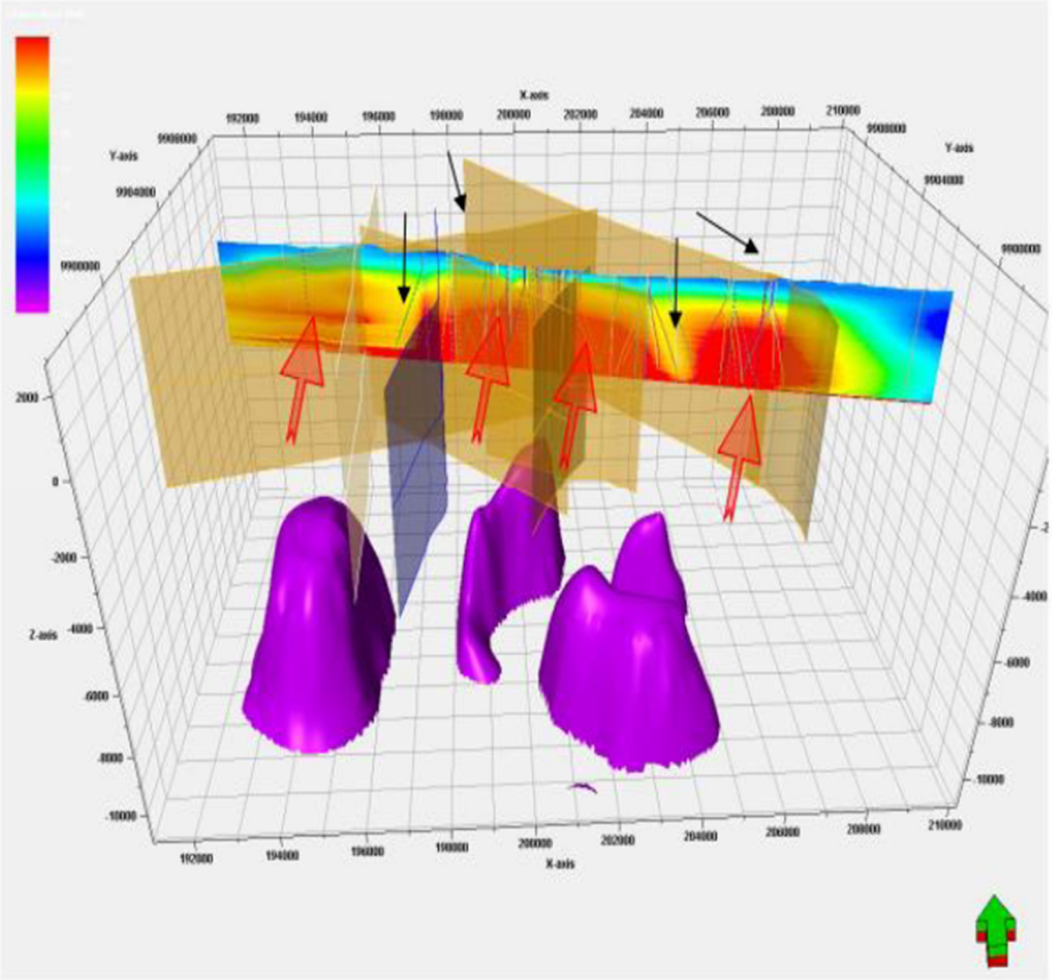

FIGURE 3: Revised conceptual model of the Olkaria geothermal system (Saitet et al., 2016); black arrows pointing downwards denote the recharge direction whereas the red arrows pointing upwards indicate the upflow zones

largely influenced by the structural features in the area, most notably the east-northeast trending Olkaria fault and the northwest trending Gorge Farm fault.

1.4 Overview of Olkaria Well OW-737

Well OW-737 is a step-out well in the Olkaria Northeast sub-field (Figure 4). It is identified by the following geographical coordinates: Easting 202092.4432, Northing 9906622.034 (WGS-84). It is at an elevation of 2162.22 m. It is a vertical well drilled to 2990 m depth from the cellar top (CT). The well was spudded on August 14th, 2016 and completed on November 22nd, 2016. An anchor casing of 13⅜" and a production casing of 9⅝" were set at 292 m CT and 1192 m CT respectively. The purpose of the well was to appraise the area in the eastern and northeastern part of the Northeast sub-field and to establish the extent of the geothermal system.

During drilling, rock cutting samples were collected at either 2 or 4 m intervals based on the amount of rock cuttings recovered. Rock cuttings provide an insight into the subsurface geological parameters related to the geothermal reservoir, such as the permeability and alteration type, intensity of alteration and its significance, rock types and their competencies. Upon completion of drilling, completion tests were undertaken to determine reservoir parameters such as permeability, transmissivity and aquifer locations.

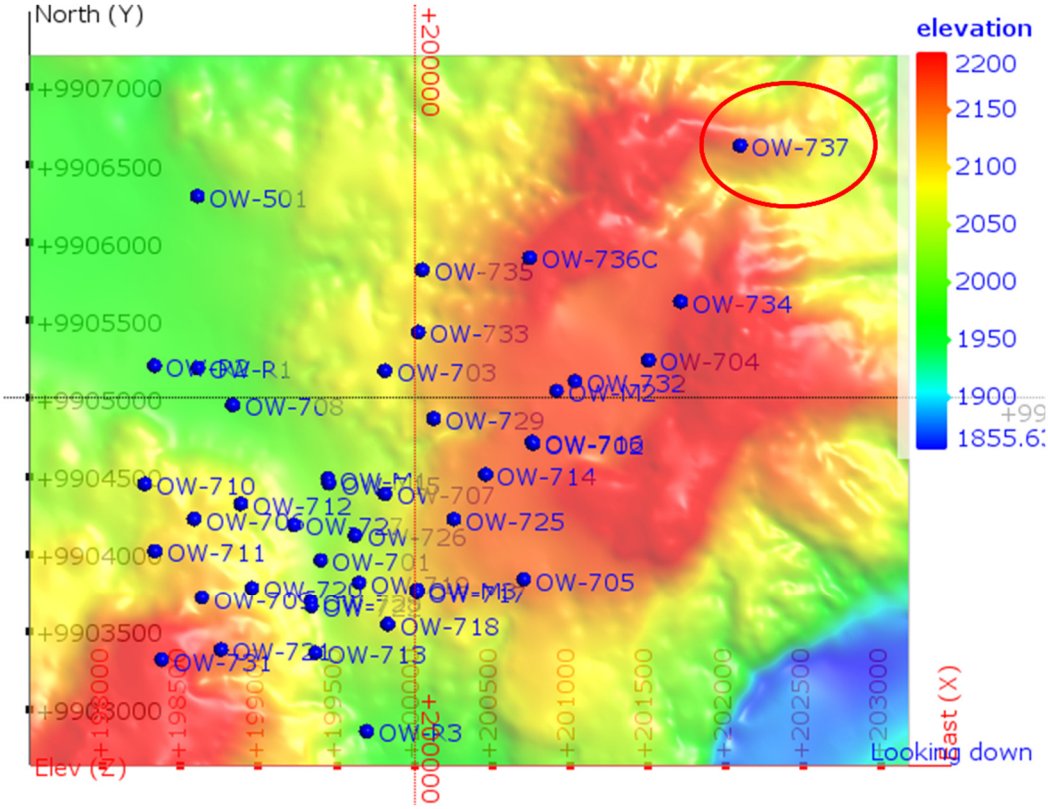

FIGURE 4: Map showing the location of the study well, Olkaria well OW-737 (circled in red) in the Northeast sub-sector of Olkaria geothermal field

The main objective of this study is to use the available borehole data, including drill cuttings, drilling parameters such as ROP (Rate of Penetration), WOB (Weight on Bit) and RPM (Rotation per Minute), reservoir temperature profile data and surface geology data to create an understanding of the geothermal reservoir parameters of OW-737 and how they contribute to the geothermal behaviour of the well. Specific objectives include:

(i) Analyse the drill cuttings to establish a lithostratigraphic sequence, characterize their properties and how they relate to the geothermal parameters.
(ii) Analyse hydrothermal alteration minerals to understand the water rock interaction and the significance of the minerals in relation to permeability and temperature.
(iii) To deduce the thermal regime that exists in OW-737 and its stability through time.
(iv) To correlate the lithostratigraphy of OW-737 with wells in the vicinity such as OW-732, OW-734, OW-735 and OW-736C to establish a resemblance in terms of structural controls and proximity to heat sources.

2. GEOLOGY

2.1 Structural evolution and tectonic settings

The geology and the tectonic setting of the Olkaria volcanic complex is related to the evolution of the EARS and the Kenya rift, but the driving force of the rifting process is provided by convection within the asthenospheric mantle (Marshall et al., 2009). The opening of the Kenya rift began with volcanism in the Miocene period. The total volume of eruptive rocks associated with the rifting is estimated to be more than 220,000 km^3 (Baker, 1987). Miocene volcanics were subsequently faulted and then followed by massive and extensive Pliocene eruptions of trachytic ignimbrites in the central area of the Kenya Rift to form the Mau and Kinangop tuffs.

A second faulting episode followed the ignimbrite eruptions, which resulted in the formation of the graben structures known today, as well as fissure eruptions of trachyte, basalts, and basaltic trachyandesites (Baker et al., 1972). Plateau rocks that filled the developing graben were then block faulted to create high angle normal faults within the rift floor. Apparently, the fractures served as conduits for the Quaternary volcanic activity of mafic to felsic composition (Ebinger and Sleep, 1998). The most intense volcanic activity occurred within the central sector of the rift, where the volcanic succession is thought to be around 5 km thick. This thickness is estimated from seismic data (Simiyu and Keller, 1997), stratigraphic correlation (Baker et al., 1972), and information from geothermal wells drilled in the Greater Olkaria Geothermal Area (Lagat, 2004).

The geological structures of Olkaria, as illustrated in Figure 5, show structural faults trending in NE-SW, NW-SE, N-S, NNE-SSW and ENE-WSW directions. The most notable structural feature is the ring fault structure confined to the Domes sub-field. This ring fracture has been defined by the alignment of the domes that are visible on the surface. Other structural features include the Ol'Njorowa gorge, which is attributed to a catastrophic outflow of Lake Naivasha (Clarke et al, 1990), leaving exposures of volcanic plugs and felsic dykes that contribute to an understanding that the gorge formation is structurally controlled. The Gorge farm fault is also a distinct structural feature in the Olkaria volcanic complex. It initiates at the end of the ring fault structure in the Domes field and cuts through the Northwest field in a NW direction all the way past Oloiden bay of Lake Naivasha.

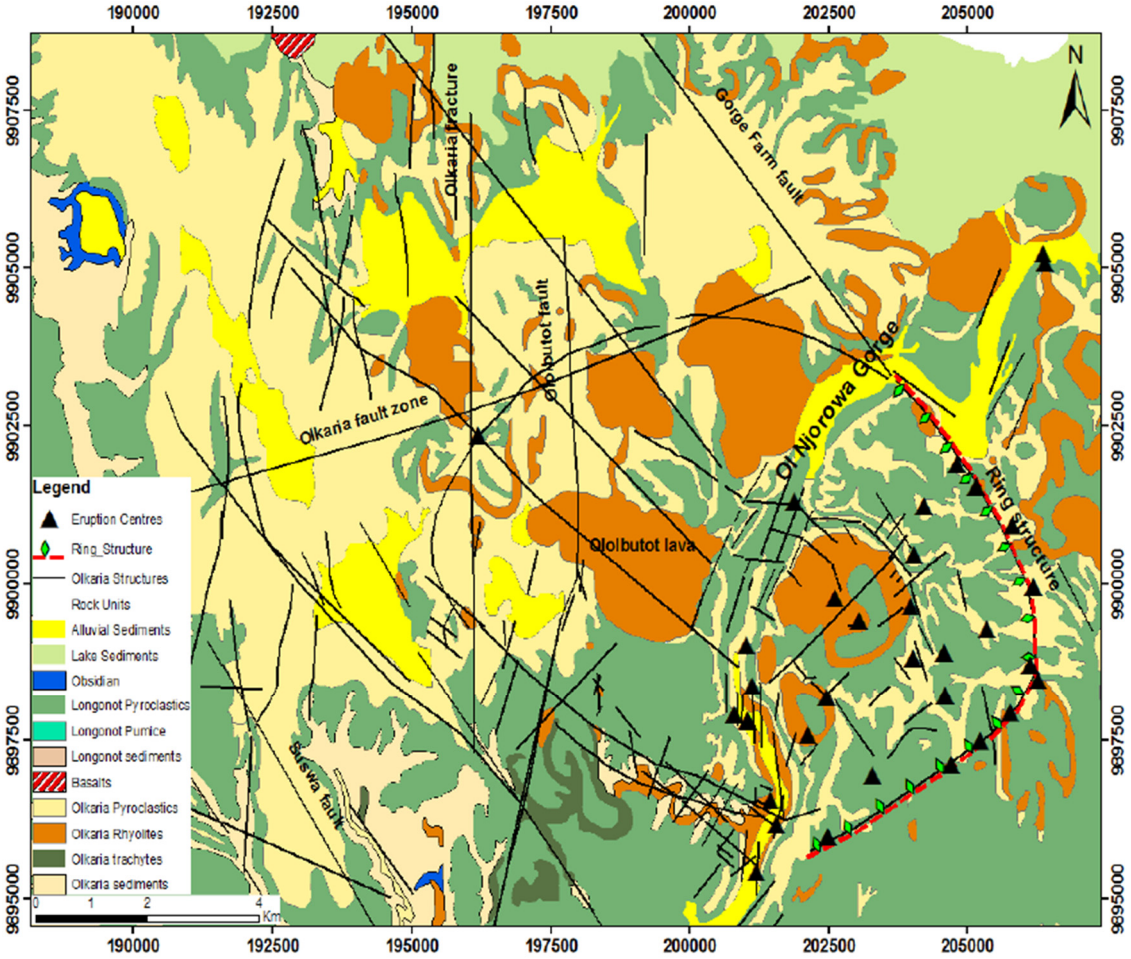

FIGURE 5: Geological and structural map of the Olkaria volcanic complex and the surrounding area (modified from Clarke et al., 1990)

Other important, prominent structural features are the Olkaria fault that trends ENE-WSW and the N-S trending Olkaria fracture and Ololbutot fault that are intersected by the Olkaria fault in the East, Northeast and West sub-fields, where the faults are prominent. In the Domes, however, the faults are

indistinct, which is attributed to a thick pyroclastic cover (Lagat, 2004; Okoo, 2013). From the field relationships, the NW-SE and WNW-ESE faults are thought to represent the oldest fault system and they link the parallel rift basins to the main extensional zone (Wheeler and Karson, 1994).

2.2 Lithostratigraphy

The Olkaria volcanic complex is a multi-centred complex dominated by peralkaline rhyolitic domes and lava on the surface (Marshall et al., 2009). Eruption centres, which occur as steep-sided domes, are the sources of the lava flows, which characterize the geology of Olkaria. The surface geology of Olkaria has been described to be comprised of pumice lapilli, ash deposits, pyroclastic deposits and comenditic lavas (Clarke et al., 1990). There is also a contribution of pyroclastic deposition from the Longonot and Suswa volcanic centres that were also active during the evolution of Olkaria volcanic complex, although it has not been quantified (Clarke et al., 1990). Figure 5 shows the surface geology and how different formations are distributed in the Olkaria geothermal field.

Evidence from geothermal drilling has revealed the subsurface lithostratigraphy of the Olkaria geothermal field to be comprised of six main groups, namely: Proterozoic 'basement' formations, Pre-Mau Volcanics, Mau tuffs, Plateau Trachytes, Olkaria Basalts and Upper Olkaria Volcanics (Omenda, 2000 and Lagat, 2004). The Upper Olkaria Volcanics are the uppermost group in the stratigraphic order. They are of mid Pleistocene to Recent age, dated 0.95 Ma (Omenda, 1998). Pyroclastics and comendites characterize the lithology series of this group along with minor interbeds of basalts and trachytes. They also consist of ashes from Longonot and Suswa and minor trachytes and basalts (Clarke et al, 1990; Omenda, 1998). The Ololbutot lavas, that are much younger and are dated at 180$\pm$50 years, form part of this group. They extend from the surface to about 500 m depth, where they are underlain by the Olkaria basaltic group. The Olkaria basalt group is Pleistocene in age, and consists of basaltic lavas with thin intercalations of tuff, rhyolite and trachyte. Its thickness varies from 100 to 500 m and the formation appears to be extensive in the East, Northeast and Domes fields, while it is absent in the West field (Okoo, 2013; Otieno, 2016). Reservoir modelling (Haukwa, 1984; Ambusso and Ouma, 1991) and hydrothermal alteration studies (Browne, 1984; Leach and Muchemi, 1987; Muchemi, 1992; Omenda 1998; Okoo, 2013) suggest that this formation forms the cap-rock of the Olkaria geothermal system.

The Plateau trachytes are of Pleistocene age and comprise trachytic lava with intercalation of basalts, tuff and rhyolites. They form the reservoir rock in the East, Northeast, Southeast and Domes fields. The formation thickness is in the range of 1000-2600 m (Odongo, 1986; Omenda, 1994, 1998; Lagat, 2004).

The Mau tuffs are beneath the Plateau trachyte and are the oldest formation dated at 3.4-4.5 Ma. The thickness of the Mau Tuffs is over 2600 m. This formation is characterized by consolidated ignimbrites (Omenda, 1994; 1998) and it has been encountered in boreholes in the west fields (Northwest and Southwest) in the area west of Olkaria Hill, while it is absent in Olkaria East due to an east dipping, high angle normal fault that passes Olkaria Hill (Omenda, 1994, 1998). The Mau Tuffs form the reservoir rock in the west fields (Lagat, 2004 and Victor, 2013). The Pre-Mau volcanics formation is dated to be older than 4.5 Ma and consists of trachyte, basalt and ignimbrites of unknown thickness.

The Proterozoic basement has an approximate thickness of 5000-6000 m according to reflection seismic, gravity and geological studies (Simiyu and Keller, 1997). Furthermore, the seismic and gravity studies indicate the presence of high-density magmatic intrusions in the metamorphic 'basement' rock as concurred by Baker and Wohlenberg (1971). The Proterozoic basement comprises metamorphic amphibolite-grade gneisses, schists and associated marble and quartzites (Shackleton, 1986; Mosley, 1993; Smith and Mosley, 1993; Simiyu and Keller, 1997). This formation has not been reached with drilling at the Olkaria geothermal field. Table 2 shows the summarized stratigraphic sequence with depth from the surface to the basement.

TABLE 2: Summarized stratigraphic groups of Olkaria formations

No.	Group	Lithology	Thickness (m)	Characteristics
1	Upper Olkaria	Comendite lavas and their pyroclastic equivalents, ashes , minor basalts	Surface-500 m	Superficial
2	Olkaria basalt	Basalt flow, minor pyroclastics and trachytes	100-500	Cap-rock
3	Plateau trachyte	Trachytes with minor basalts, tuffs and rhyolites	1000-2600	Reservoir
4	Mau tuffs	Consolidated ignimbrites	>2600	Reservoir
5	Pre-Mau volcanics	Trachytes, basalts, ignimbrites	unknown	Reservoir
6	Proterozoic	Gneisses, schists, marbles and quartzites	5000-6000	Basement

3. METHODOLOGY

3.1 Sampling and analytical techniques

A major component of this study is the analysis of drill cuttings sampled during the drilling of OW-737. Drill cuttings are rock chips that are lifted to the surface with the aid of drilling fluids during drilling. Drill cuttings were sampled at 2 m intervals for the entire depth of well OW-737 (0-2990 m), but where samples were scanty a 4 m interval was adopted. The depths where no returns were recovered were also recorded. Preliminary analysis was done at the rig site. Below, analytical techniques are listed, which were applied to obtain information about the lithology, hydrothermal alteration minerals, permeability types and paragenetic sequences.

3.1.1 Stereoscope microscopy analysis

This analysis involved visual observation of the drill cuttings with the aid of an analytical binocular microscope to obtain information on the lithological composition and alteration mineralogy using the physical or chemical properties of the minerals. Properties used to identify minerals and rocks include colour, crystal habit/form, grain size and texture, structure and effervescence and general composition. Also noted in this analysis are vein fillings, alteration and the oxidation intensity of the rock cuttings. The sample preparation procedure entailed obtaining a representative rock cuttings sample, washing it in fresh water, placing it in a small plastic box filled with water and onto the mounting stage of the binocular microscope, where it was examined. An Olympus SX16 model binocular microscope was used for this analysis. The results of the visual observations were documented simultaneously.

3.1.2 Petrographic microscopy analysis

The petrographic analysis entailed the preparation of thin sections from the rock cuttings, through the process of shattering, lapping and obtaining the recommended thin section slide. Petrographic microscopy makes use of transmitted polarized light and assists in identifying minerals by making use of their optical properties and distinctive characteristics such as colour, cleavage, relief, birefringence, twinning and interference colours. The minerals are identified through observations under plane polarized light (PPL) and crossed polars (XPL) as each mineral has different optical properties. The basis of this type of analysis is to obtain extra details that were not available in the binocular analysis. It is particularly reliable in the identification of the rock type, paragenetic sequences of hydrothermal alteration minerals and the extent to which primary minerals have been altered. Therefore, 53 samples identified at different depth intervals of the well were selected. In this analysis, a Leica petrographic microscope was applied. The results were then incorporated to the binocular analysis results.

3.1.3 X-Ray Powder Diffraction (XRD) analysis

X-Ray Powder Diffraction (XRD) is an instrumental technique that is used to identify fine-grained clays and other crystalline materials that are not easily identified with other techniques. It is a basic technique for clay mineral analysis (Moore and Reynolds, 1989). Sample preparation procedures involve the careful washing of each selected sample in distilled water. Samples of about 2 g are put in a glass test-tube, the tube is nearly filled with distilled water and put in a mechanical shaker. The sample is shaken for about 4 hours. The suspended clay-slurry is left to settle for about 10 minutes and then transferred onto a glass-slide, using a pipette. The sample is left overnight to dry in ambient temperature and humidity. The sample is measured after complete drying and recorded as UNT (untreated) and after the measurement, the sample is placed inside a closed desiccator, where the container above is filled with ethylene-glycol. The sample is left in the ethylene-glycol fume for 24 hours and then measured and recorded as GLY (glycolated). Finally, the sample is heated in a furnace for about 1 hour at 550°C and after cooling, measured again as HIT (heated).

Each sample is measured from $2\Theta = 2–14°$, in 0.02° increments (steps) and measured for 1 second in each step. The set-up is saved in a parameter file *leir-a.dql.* Each measurement takes about 20 minutes. The X-ray beam is confined using a 0.5° divergence and receiving slits. The equipment used is a Bruker AXS D8 Focus, that produces Cu kα radiation with 1.54 Å wavelength at 40 kV and 40 mA. The detector used is a NaI scintillation counter.

The results of the XRD analysis are presented in the form of computer scans or spectrographs for the set of the three measurements, untreated (UNT), glycolated (GLY), and heated (HIT), which are viewed superimposed using Bruker, Diffra.Eva, a special software for XRD display. The spectrographs display the position of the diffraction maxima, the peak intensities and the intensity distribution as a function of diffraction. Clay interpretation stages were carried out using the PowDLL and DiffracPlus EVA softwares. The former is used to convert the XRD Shimadzu data type to Brucker type, while the latter is used to evaluate the different clay types. The interpretation of the clay type is accomplished by comparing the d-spacing from the sample with peaks and relative intensities from a very large set of standard reference patterns provided by the International Centre for Diffraction Data (ICDD). In this clay analysis, 15 rock cuttings samples were selected from depths of interest and the results are presented in Appendix I.

3.1.4 Fluid inclusion analysis

This type of analysis involves the identification of fluid inclusions in crystals of minerals such as quartz, prehnite or calcite. In particular, it provides valuable data not only on the temperature and pressure in specific geothermal settings, but on the chemistry as well. In this study, calcite samples were handpicked from samples taken at 1410-1458 m depth. A total of 80 measurements were made from two calcite samples. The purpose of this analysis is to determine the temperature of the geothermal system through the analysis of the homogenisation temperature (Th), which is related to the temperature of the geothermal system at the time the fluids are trapped as inclusions in the crystals and can thus provide information on whether the system is cooling, in equilibrium, or heating up, when compared with the present day formation temperature. The crystals are glued onto a glass slide and polished using different grades of polish paper. Once the crystals have been polished to the required thickness of approximately 70 microns, the glass slide with the crystal is placed in a beaker and enough acetone is added to cover the glass slide. The beaker is then placed in an ultrasonic cleaner for a few minutes or until all the glue has dissolved from the glass and the crystals have been freed. The same procedure is then repeated for the polishing of the other side of the crystal. The crystal sample is then mounted in a Linkam THS MG 94 heating stage and observed in a petrographic microscope while it is heated gradually until the homogenization temperature (T_h) is obtained. This happens, in the case of liquid rich fluid inclusions, at the point when the liquid and the coexisting fluid inclusion bubble coalesce and the bubble disappears. Detailed procedures of fluid inclusion analysis are found in Roedder (1984) and Shepherd et al. (1985).

4. RESULTS

4.1 Lithostratigraphy

Incorporating both the analytical binocular and petrographic microscopy techniques, the rock cuttings analysis resulted in the lithological units of OW-737 from the surface to 2998 m CT being clustered into five lithological series that are further divided into subunits based on mineralogical composition and textural properties (Table 3). With increasing depth and varying thicknesses the lithological series are: pyroclastics, rhyolites, basalts, trachytes and microsyenite intrusions. Zones with no cutting returns have been incorporated into the lithological units. By doing this, an assumption is made that the lithological units are continuous, with the exception being the pyroclastic unit which has a loss zone of 174 m. The lithological units have also been correlated with the lithostratigraphic groups of the Olkaria volcanic complex (Omenda, 2000).

TABLE 3: Simplified lithostratigraphy of OW-737

No.	Lithology series	Depth interval (m)	Thickness (m)	Lithology Sub-series		Depth interval (m)	Loss zones (m)	Olkaria stratigraphic group
1	Pyroclastics	0-34	34	Pyroclastic		0-34		
2	Rhyolites	34-568	534	Rhyolite	I	208-248	34-208 234-248	Upper Olkaria volcanics
				Rhyolitic tuff	I	248-318	252-314	
				Rhyolite	II	318-490		
				Rhyolitic tuff	II	490-568		
3	Basalts	568-782	214	Basalts	I	568-612		Olkaria basalts
				Trachyte	I	612-680	612-658	
				Basalts	II	680-694		
				Rhyolitic tuff	III	694-714		
				Rhyolite	III	714-732		
				Basalts	III	732-782	766-782	
4	Trachytes	782-2882	1186	Trachyte with basalt dikes	II	782-1448 1278-1280 1294-1296 1418-1440	858-872 948-978	Plateau trachyte
				Trachytic tuff and trachyte	I	1448-1540		
				Trachyte w. rhyolitic and basaltic dikes	III	1540-1892 1644-1656 1692-1760 1806-1826	1668-1692	
				Brecciated tuff and trachytic tuff	II	1826-1968		
				Trachyte	IV	1968-2882	2594-2634 2642-2720 2724-2792 2794-2830	
5	Syenite	2882-2990	108	Microsyenite		2882-2990		Olkaria intrusive

4.1.1 Pyroclastics (0-34 m depth)

The pyroclastics unit forms the top of the lithological sequence of OW-737. It is generally light coloured with variable mixed shades of grey and yellow brown. It is composed of loose and unconsolidated volcanic ash, pumice lapilli and lithic fragments of obsidian, tuffs and rhyolite. The colour and variation

in the components in this series attests to the notion that the Olkaria pyroclastic deposits are to a certain extent composed of air fall deposits from the Suswa and Longonot volcanos (Clarke et al., 1990; Musonye, 2015). The eruption of Longonot and Suswa dispersed air falls over Olkaria and westwards to areas beyond Maiella and Sekuttiek towards the west rift escarpment. The Longonot and Suswa tephras are grey while the Olkaria tephra is light yellow brown. The provenance of the pyroclastic deposits in Olkaria can be resolved through petrochemical analysis. However, it is evident from the surface geology, that the three volcanic eruption centres have a similar surface lithology cover. It is not hydrothermally altered, only oxidized due to the interaction of oxygenated groundwater with the iron content of the deposits. The unit as sampled from the surface is 34 m thick. In correlation with the Olkaria lithostratigraphic column, it belongs to the Upper Olkaria volcanic group and is therefore the youngest.

4.1.2 Rhyolite series

The rhyolite series is the formation below the pyroclastics with a thickness of 534 m. Based on mineralogical composition and textural properties, this series is found to be mainly rhyolitic lava intercalated with tuff of rhyolitic composition that is referred to as rhyolitic tuff. This rock series suffers from large zones of circulation losses, e.g. at its contact with the pyroclastics. The total depths with loss of return accounts for almost 50% (256 m) of the entire thickness of the series. This could be attributed to the heterogeneity and blocky nature of the formation. The rhyolite series belongs to the Upper Olkaria volcanic stratigraphic group and has been divided into four subseries that are described below:

Rhyolite I (34-248 m depth): This formation is light grey to white in colour with minor brownish colouration. The texture is fine-grained to fairly microcrystalline, composed primarily of quartz and sanidine with euhedral to subhedral quartz phenocrysts. Plagioclase, arfvedsonite and riebeckite are also present but mostly as accessory minerals. It also shows a distinctive spherulitic texture in which micro crystals of quartz and feldspar are clustered together and radiate from a common focal point. This texture is especially pronounced at shallow depths. A glassy matrix with glass shards showing flow direction is also common at the contact with the pyroclastics and upon alteration it has been devitrified. The brownish colouration is attributed to oxidation. At shallow depths it appears to be fresh to weakly altered with alteration minerals such as oxides, zeolites and calcites infilling vesicles.

Rhyolitic tuff I (248-318 m): The rhyolitic tuffs occur as intercalations between the rhyolitic sub-series and have been divided into two. They are rhyolitic in composition, hence referred to as rhyolitic tuff. They differ in texture to the rhyolite in that they are heterogeneous and contain lithic fragments of quartz and sanidine feldspars in a fine-grained matrix. They appear fresh to weakly altered with alteration minerals such as clays, oxide, calcites and zeolites infilling vesicles.

Rhyolite II (318-490 m depth): This formation shows similarities in rock properties with rhyolite but there is an abundance of arfvedsonite and riebeckite amphibole that is intergrown with sanidine feldspar. Additionally, it is more holocrystalline and the spherulitic texture is distinct. The alteration of the formation has resulted in minerals such as secondary quartz, zeolites, calcites and oxides.

Rhyolitic tuff II (490-568 m): This unit is similar in composition to rhyolitic tuff I but it is partly holocrystalline with a flow banding texture. Occasionally porphyritic and vesicular.

4.1.3 Basalt series

The basalt series occurs below the rhyolitic series and is a 214 m thick series of lava flows. Basalt is the dominant lithological unit, which is intercalated with rhyolitic tuff and trachytic lava and forms three basalt sub series. The basalt series collectively belongs to the Olkaria volcanic stratigraphic group. The characteristics of the basalt series are defined below.

Basalt I (568-612 m): This formation is variably brown to dark grey to black, fine grained and holocrystalline lava. The basalt is occasionally porphyritic with plagioclase and clinopyroxene

phenocrysts with indistinct anhedral olivine that show significant alteration. Plagioclase feldspar also occurs as elongated subhedral phenocrysts. The basalt is vesicular with moderate alteration represented by zeolites, calcites, oxides, chalcedony and secondary quartz with significant chloritization.

Trachyte I (612-680 m): Trachytes in this series have been categorized as trachyte I and II and they occur as intercalations between basalts and rhyolitic tuff. Trachyte I intercalates basalt I and basalt II while trachyte II occurs in between rhyolitic tuff III and basalt III. Trachytes in this series are crystalline and fine grained. They are also massive with sanidine feldspars occurring as large phenocrysts that are euhedral to subhedral.

Basalt II (680-694 m): This unit is notably similar to the basalt I composition. However, it is distinct because of the holocrystalline groundmass and additional alteration minerals such as albite.

Rhyolitic tuff III (694-714 m): In this series, rhyolitic tuff occurs as thin layers of 20 m thickness, occurring between basalt II and trachyte II. It is grey and fine grained, poorly crystalline to massive. It is quartz and sanidine feldspar rich with some minor pyroxenes and feldspar microlites. The groundmass is partly glassy and accessory minerals such as titanite and hematite are identified.

Rhyolite III (714-732 m): This unit is aphyric and crystalline and primarily composed of sanidine feldspar and quartz. The pyroxenes, in many cases aegerine-augite, and riebeckite amphiboles, occur as accessories that are occasionally noted embedded in a feldspar rich groundmass. Flow texture is exhibited in some fragments.

Basalt III (732-782 m): This basalt unit is dark brown and holocrystalline and has the same composition as basalt I and basalt II, although calcites are more abundant as alteration minerals.

4.1.4 Trachytes series

Trachyte II with basalt dikes (782-1448 m depth): The trachyte is the main lithological unit that has intrusions of basalt. The trachyte is characterized by being light grey to whitish grey colour, felsspar rich, fine to medium grained with porphyritic texture. It is rich in alkali feldspars, mostly sanidine. Pyroxene crystals are occasionally noted embedded in a feldspar rich groundmass. Some of the fragments exhibit flow texture. Alteration intensity is also high as it is in this zone that high-temperature alteration minerals such as epidote and actinolite are encountered. This group fits into the category of the plateau trachyte with Olkaria intrusions.

Trachytic tuff I (1448-1540 m depth): The trachytic tuff and trachyte in this zone appear brownish grey to light grey, moderately to highly porphyritic with a fine-grained groundmass. Primary minerals include sanidine feldspars and minor pyroxenes. The feldspar shows zoning and alteration. This zone is highly altered to high-temperature alteration minerals such as epidote and prehnite. Other alteration minerals in abundance are calcites and pyrite. Overprinting of epidote by calcite is also notable in this zone.

Trachyte III with rhyolitic and basaltic dikes (1540-1892 m depth): The mineral composition and texture is similar to trachyte II, but becomes earthy brown, oxidized and glassy where it is brecciated, e.g. at 1826-1840 m, altering the texture of the trachyte, with slickensides marks clearly observable in thin section. Within this zone, intrusions occur as rhyolitic intrusion I (1644-1656 m) and rhyolitic intrusion II (1692-1760 m).

Brecciated tuff and trachytic tuff II (1826-1968 m depth): Trachytic tuff is the dominant lithology and it is fine grained, slightly porphyritic with sanidine that is fairly altered and oxidized. It also appears massive. Where brecciated, the formation consist of earthy brown, glassy and massive or vesicular agglomerate which is micro-fragmented. Alteration minerals such as epidote, prehnite, wollastonite and actinolite occur as replacement of sanidine feldspar and also as vesicle filling.

Trachyte IV (1968-2882 m depth): This formation is characterized by a light grey to whitish grey colour, it is felsic rich, fine to medium grained with porphyritic texture. It is rich in alkali feldspars, mostly sanidine laths. Aegerine augite pyroxene crystals are occasionally noted embedded in a feldspar rich groundmass. Some of the fragments exhibit flow texture as observed in thin section. Alteration minerals such as quartz, epidote, prehnite, wollastonite and actinolite also continue to occur as replacement and vesicle fillings but with a decline in abundance with depth.

4.1.5 Intrusions

OW-737 is characterized by intrusive phases that occur as dikes at variable depths or deep seated intrusions. Intrusions occur either as thin layer or possibly as dikes in which case they can be exemplified as basaltic and rhyolitic intrusions. Microsyenites can be referred as deep seated due to their depth and thickness.

Basaltic intrusions intrude the trachyte III series at variable depths and have been classified in the order of lithological sequence as basalt intrusion I (1278-1280 m), basalt intrusion II (1294-1296 m), basalt intrusion III (1418-1440 m) and basalt intrusion IV (1806-1826 m). They are dark grey to black, fine grained to holocrystalline and moderately porphyritic with intermittent plagioclase feldspar phenocrysts. They are also rich in opaque minerals and euhedral crystals of augite pyroxene. Alteration is significant with plagioclases altered to clays, epidote and calcite while opaque minerals are altered to titanite and hematite.

Rhyolitic intrusions: They intrude the trachyte III series and have been categorized into rhyolitic intrusion I (1644-1656 m) and rhyolitic intrusion II (1692-1760 m). They are grey, fine grained and quartz and feldspar rich with minor plagioclase feldspars, slightly porphyritic with small sized sanidine feldspar phenocrysts. Hornblende and riebeckite occur as accessory minerals. The spherulitic texture is also recognizable.

Microsyenite: They are intrusive equivalents of trachyte appearing as white to grey in colour, fine- to medium-grained crystalline rock. The microsyenite is moderately porphyritic with the matrix composed of elongated crystal laths of sanidine feldspar. Other constituents are quartz with pyroxene and arfvedsonite-riebeckite as mafic constituents. The latter are conspicuous with blue colour and elongated crystals. They occur at 2882 m and extend to the total depth with a thickness of 108 m, though there are a few metre depths with loss of returns. This unit therefore belongs to the Olkaria intrusions and they are much younger in the stratigraphic column intruding the Plateau trachyte.

4.2 Hydrothermal alteration mineralogy

Hydrothermal alteration refers to the changes in the mineralogy of the rock due to changes in the prevailing physio-chemical conditions. As a result, the primary minerals become unstable and respond by altering to a secondary phase, giving rise to precipitation of secondary minerals. Hydrothermal alteration is basically a change in the mineralogy as a result of the interaction of the rock with hot water fluids, called “hydrothermal fluids” (Simmons and Browne, 2000; Lagat, 2004). Fluids are carriers of metals in solution, either from a nearby source, or from leaching out of nearby rocks, which, depending on the water rock interaction and the temperature regimes, form different hydrothermal alteration mineral assemblages. Factors influencing the distribution and the kind of hydrothermal mineral assemblages therefore include: the permeability and composition of the host rock, composition of circulating fluids, temperature, pressure and duration of hydrothermal alteration (Browne, 1978). These factors are largely independent, but the effects of one or more of the factors can exert a dominant influence on the location and extent of hydrothermal alteration (Browne, 1978, 1984).

When rocks are hydrothermally altered, the primary minerals yield specific alteration replacement products (Table 4) (Browne, 1984). Alteration products from primary minerals are related to their

crystallization order in the Bowen reaction series. Table 4 indicates the minerals that crystallize first, for example olivine and pyroxene are the most susceptible to alteration while K-feldspar e.g. (sanidine, microcline) that crystallizes last is the least susceptible. Volcanic glass is the phase that is most susceptible to alteration. The corresponding products are also indicated in Table 4. During alteration, the original colour, texture and form are lost partially or totally depending on the prevailing physiochemical conditions. However, Kristmannsdóttir (1979) in her study of various geothermal fields in Iceland, indicated that it is possible to correlate temperatures with selected alteration minerals in systems that have remained in a steady state of thermal equilibrium over a period of time.

TABLE 4: Primary minerals, their alteration products and order of replacement as observed in the study wells (modified from Browne, 1984)

	Primary minerals	Alteration products
Most susceptible	Volcanic glass	Zeolites, clays, chalcedony, quartz, calcite
⇓	Olivine	Chlorite, clays, calcite
⇓	Pyroxenes, amphiboles	Chlorite, illite, quartz, pyrite, calcite
⇓	Plagioclase	Calcite, albite, quartz, epidote, titanite
Least susceptible	Sanidine	Adularia, chlorite, illite, calcite
	Fe-Ti oxides	Titanite, pyrite, hematite

Rock cuttings were analysed using binocular and petrographic microscopes to identify hydrothermal alteration minerals and XRD was used to identify clay minerals. The hydrothermal minerals are known to provide useful information, on e.g. paleo-temperature, permeability and the thermal regime of the geothermal reservoir, and they have been applied to understand the geothermal reservoir properties.

Types of hydrothermal alteration minerals were noted as per depth of occurrence, as well as the abundance of selected minerals, the alteration intensity and properties such as crystallinity, crystal form/habit, and nature of emplacement, whether depositional in matrix or vug/vein/fracture/vesicle, or as replacement. Figure 6 illustrates the types of alteration minerals identified in OW-737.

The hydrothermal alteration minerals of OW-737 are classified as follows: oxides (magnetite, hematite and limonite) calc-silicates (prehnite, zeolites, epidote, titanite, wollastonite and actinolite), clays (chlorite, smectite and illite), secondary feldspars (albite), silica minerals (chalcedony, quartz), carbonates (calcites and siderite), sulphides (pyrite) and fluorite. Analysis shows that the degree of alteration intensity increases with depth and the alteration minerals have been formed by processes such as replacement, dissolution, leaching, and recrystallization or direct precipitation in vugs/vesicles, veins or fractures. There is an overprint alteration or retrograde alteration noted from the sequence of association of low- and high-temperature alteration minerals. Hydrothermal alteration minerals are described below.

4.2.1 Hydroxides-oxides (limonite, hematite and magnetite)

The presence of iron oxide minerals can indicate the presence of cool, oxygenated water. It also indicates that the zone is fractured and permeable, allowing the ingress of oxygenated waters that cause staining of the iron component of the rock

Limonite is a hydrated iron oxide mineral and is observed as yellow orange to reddish brown. It is formed in association with the hydration of hematite or magnetite and is confined to the depth from 248 to 400 m.

Magnetite as an alteration product is rare in this well and occurs sporadically from 599 to 2000 m. It appears as black to brown, well-formed octahedral crystals in a thin section. It is occasionally observed to infill veins or vesicles and as disseminated grains in the rock matrix. Rock forming magnetite altered to titanite was observed at 2032 m depth.

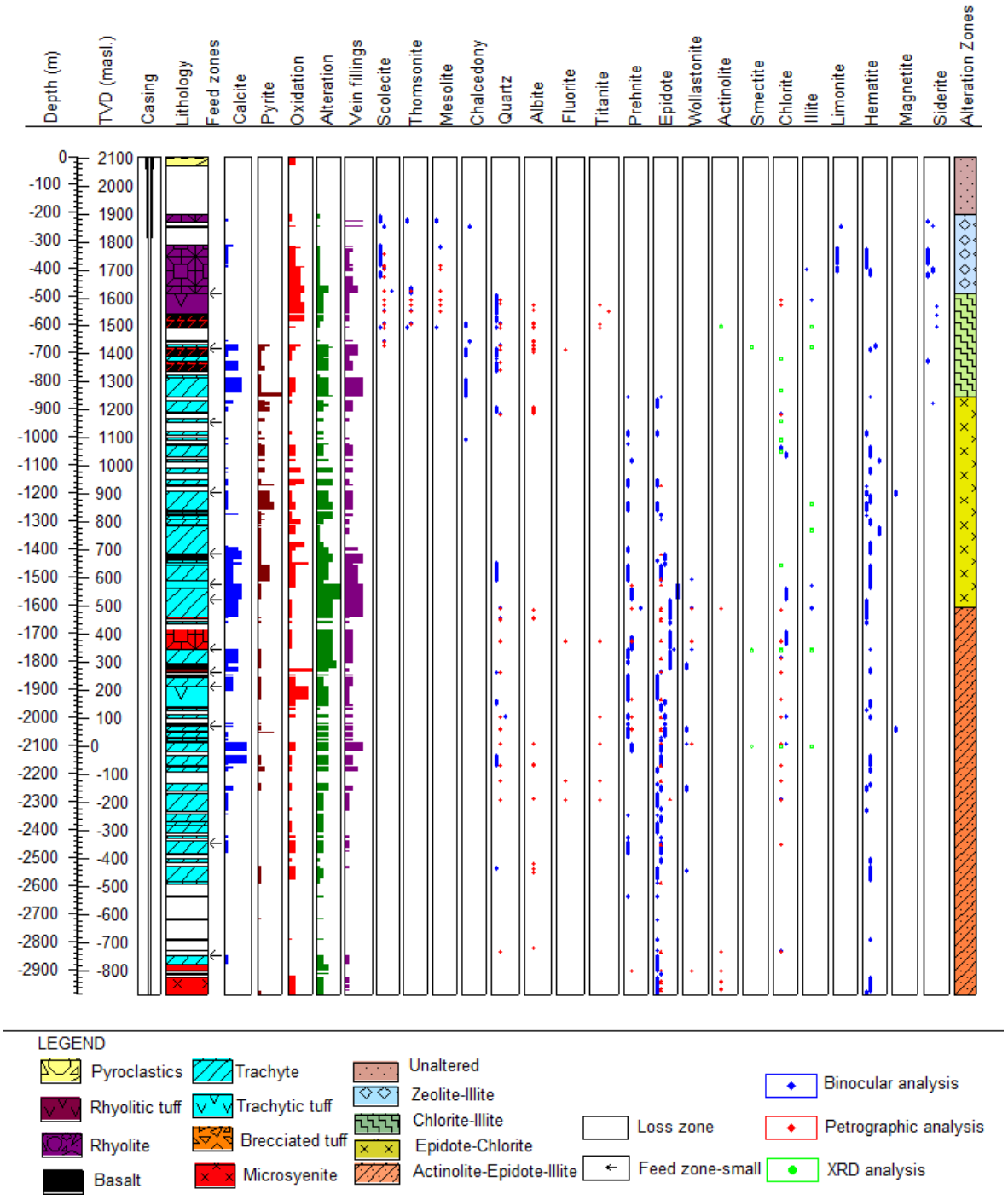

FIGURE 6: OW-737 lithology, hydrothermal minerals and mineral zones

*Hematite i*s the most abundant oxide of iron and it is common in the entire well while varying in abundance. Optically it is identified by its silver-grey, occasionally brown to reddish brown colour. It appears as disseminated minerals and to some extent as vesicle fillings. Occurrence is associated with the incursion of cold groundwater and other oxidizing conditions in a geothermal system (Brown, 1978).

4.2.2 Silica minerals (chalcedony and quartz)

Quartz, here also referred to as secondary quartz, occurs mostly as precipitates in hydrothermal open space (vesicles) and veins, occasionally replacing chalcedony. It is identified as a colourless mineral, typically euhedral to subhedral long prismatic crystals with steep pyramidal terminations. It occurs in

sequence with calcites and chlorite and occasionally with epidote. It is first recorded at 490 m depth and continues to appear intermittently to 2538 m depth. Under the petrographic microscope, it is a uniaxial mineral and easily identified by undulating extinction features, colourless with conchoidal fracturing as the most conspicuous diagnostic features. The appearance of quartz indicated an alteration temperature of 180°C.

Chalcedony occurs as vein or vesicular linings and in association with quartz and zeolites. Its first appearance is noted at 248 m depth and it occurs down to 1010 m depth. It is colourless, white, or bluish-grey with distinguishable cryptocrystalline texture and a banded concentric-like habit. Chalcedony forms at temperatures from 150°C to as high as about 180°C. This explains why it does not occur in the deeper part of the well as it probably transformed to quartz.

4.2.3 Secondary feldspar

Albite is the alteration replacement product of primary feldspar in the process referred to as albitization. It also occurs as vesicle fillings. Albite is identified in thin section by its cloudy white or greyish white colour with uneven fracturing and cleavage, low relief, multiple twinning and occasionally appearing as striated with anhedral to subhedral crystals. Its first appearance is noted replacing sanidine feldspar at 526 m depth. It becomes common between 800m and 900 m, thereafter it is intermittent.

4.2.4 Carbonates (calcite and siderite)

Calcite is the most abundant alteration mineral and observed continuously from 228 m depth to the bottom of the well. It is white in colour and was easily recognized by its reactivity with diluted hydrochloric acid. In thin section, calcite was identified by the very high birefringence and it shows three perfect cleavages (rhombohedral) and twinkling relief upon rotation of the microscope stage. In OW-737, it occurs mainly as precipitates in fractures, veins or voids. In some instances it occurs as a replacement of plagioclase feldspars, e.g. at 1278 m depth. Calcite can form through the processes associated with boiling, dilution or condensation of CO_2 enriched geothermal fluids. Browne and Ellis (1970) indicate that high CO_2 concentrations in a solution in the presence of a mineral pH buffer causes calcite to form in place of other calcium alumino-silicates.

Many studies have associated calcite presence in geothermal wells to indicate possible boiling conditions and high porosity (Browne, 1984; Omenda, 1998; Muchemi, 1992; Simmons and Christenson, 1994; Okoo, 2014). In open spaces, calcite deposits in response to boiling (Thompson and Thompson, 1996). Bladed calcite and calcite with a dogtooth structure indicates there has been high permeability in the past. Calcite is stable at large temperature ranges. However, it becomes unstable and disappears at temperatures exceeding 300°C (Simmons and Christenson, 1994; Eshagpour, 2003). The sequence in which it occurs in association with other minerals informs on the condition of the geothermal reservoir, e.g. calcite was observed to overprint epidote at 1418, 1528, 1608 and 1784 m, as shown in Figure 7, which may imply cooling.

Siderite is noted to occur from 224 to 732 m depth. It is identified in a binocular microscope by its yellow rounded aggregate that is filling vugs and veins. The presence of siderite indicates cold aquifers with temperatures less than 50°C (Eshagpour, 2003).

4.2.5 Sulphides (pyrite)

Pyrite was identified from 670 m depth and continues to variably increase in abundance from 872 to 2290 m depth where it declines in abundance again. It was easily recognized in a binocular microscope by its brass yellow metallic colour and cubic crystals. In thin section it is opaque and with a granular form. Pyrite was noted to occur either as a replacement of opaque minerals or depositional infillings in fractures, veins, vesicles or disseminations in rock groundmasses. It is observed in OW-737 that an abundance of pyrite correlates well with interpreted feed zones that also coincide with zones with abundant vein fillings, calcite abundance and increased alteration intensity, such as at 950, 1200, 1400-1550 and at 2000 m. Eshagpour,

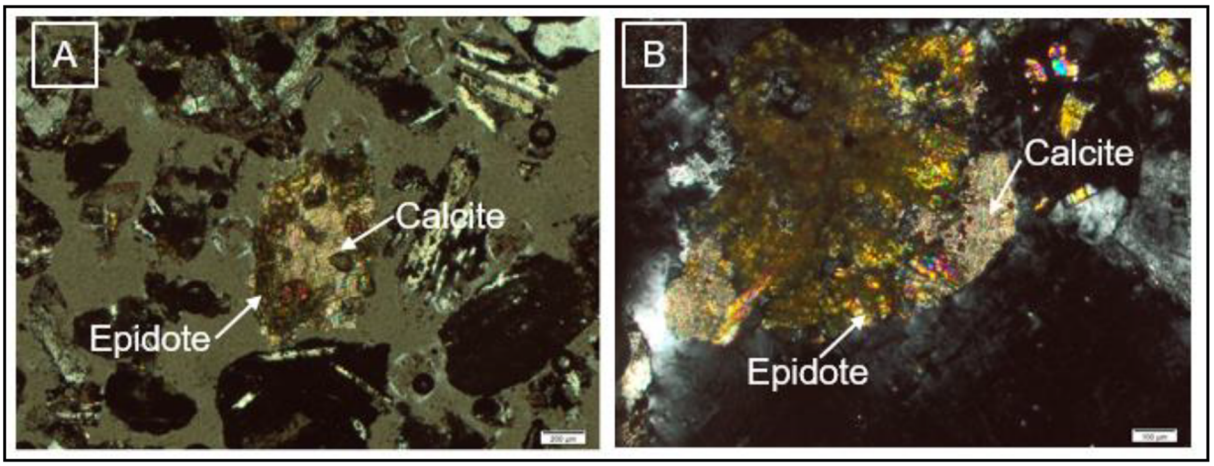

FIGURE 7: Micrograph of calcite overprinting epidote in crossed polars at (A) 1418 m and (B) 1528 m depth in OW-737

(2003) indicates that pyrite implies good permeability in the formation. However, it is not an indicator of temperature and nor of boiling regimes (Lagat, 1998).

4.2.6 Calc silicates (prehnite, zeolite, epidote, titanite, wollastonite and actinolite)

*Zeolite*s are secondary calc-silicate minerals and their occurrence is mostly temperature dependent (e.g. Bird et al., 1984). They form at relatively low temperatures (<120°C). The types of zeolites identified in OW-737 are of low-temperature types such as mesolite, scolecite and thomsonite and are confined to depths between 208 and 658 m as depositions in veins and vesicles. They are easily identified in thin section, binocular microscope and XRD. Scolecite occur as colourless tiny crystals that are clustered and appear to radiate from a common focal point. Thomsonite forms dense masses of radiating clustered minute crystals, slightly flattened with slanted ends. Mesolite occurs as thin, needle-like crystals, red to white in colour. The grains separate as they radiate away from the base, forming spiky ends. In XRD, traces of zeolites were identified at 402-404 m and 532-534 m depth. Zeolites are low-temperature deposition minerals associated with deposition temperatures between 40 and 120°C.

Prehnite is an alteration product of iron-rich mafic minerals. Its formation is associated with temperatures above 240°C. It is identified by its colourless to grey colour with a distinct vitreous–pearly lustre, strong birefringence, high relief and a characteristic bow-tie texture in thin section. It is very similar to epidote and occurs in association, but it differentiates by lack of yellow colour and pleochroism. It is first recorded at 856 m and becomes common all the way to 2640 m depth and is observed to occur both in vesicles, micro-veins and fractures.

Wollastonite is identified by being colourless and its fibrous crystals with high interference colours with a parallel extinction in thin section analysis. In binocular analysis it is seen to occur as an aggregate of white to colourless, needle-like, elongated crystals. It occurs as a vug mineral or vesicle fillings and in association with epidote, actinolite, calcite, hematite and pyrite. It is a high-temperature mineral, which represents a minimum deposition temperature of about 270°C.

Epidote is associated with high temperatures of over 230°C and forms as a replacement product of either plagioclase feldspar, pyroxenes and micas among others, or from earlier formed alteration minerals. Its first appearance indicates the top of the geothermal reservoir. The first appearance of epidote in OW-737 was noted at 856 m from where it continues to occur down to the bottom of the well. A high abundance of the mineral is noted between 1500 and 1800 m. It is easily identified in a binocular microscope by its characteristic yellowish-green to pistachio-green colour. In thin section it was identified by high interference colours in crossed nicols, while it exhibit yellow pleochroism in plane polarized light. Its mode of occurrence in OW-737 is deduced to be a replacement of plagioclase feldspar

and as a depositional mineral in void spaces. It is found to occur in association with other minerals such as prehnite, chlorite and calcite.

Actinolite is a high-temperature index mineral signifying high temperatures of above 280°C (Lagat, 2007; Gylfadóttir et al., 2011). It is first observed in a thin section at 1610 m and occurs sparingly to the bottom of the well. It is recognized by its pale green to white colour, occurring as radiating and fibrous crystal aggregates. In thin section, it is fibrous with moderate relief and shows moderate pleochroism with good cleavage. Actinolite crystals grow in vesicles as deposition minerals as well as replacing pyroxene. It is observed to form mineral associations with wollastonite and epidote. In XRD, amphibole was identified at 604 m. It is a primary mineral and is associated with Olkaria rhyolites that are rich in riebeckite and arfvedsonite, which were also identified in thin sections.

Titanite forms as a replacement of opaque minerals (Fe-Ti–oxides). It is a common mineral in this well. It was first encountered at 526 m depth and appears intermittently down to 2794 m. It occurs mainly as irregular grains but rarely as clear euhedral crystals, having acute rhombic sections. It is identified in thin sections as red-brown and somewhat cloudy, coloured crystals. Titanite occurrence indicates poor permeability in the Philippines (Reyes, 1990; Eshagpour, 2003).

Fluorite is not common in OW-737 but is identified in thin sections at varying depths by its low relief, two perfect cleavages and its pale brown to colourless colour. It is isotropic under crossed polarized light. Fluorite occurred as vein fillings. Its occurrence is limited to 686 m and between 1724 and 2292 m depth.

4.2.7 Clays

Clays are typically fine grained, hydrous, aluminium phyllosilicates characterized by sheet structures. Various clays occur as a result of argillic and propylitic alteration types that produce clays such as smectite, illite, chlorite and mixed layered clays, especially illite-chlorite and smectite-chlorite. This is in response to changes in parameters such as temperature, pressure and the chemical condition of the geothermal system. This is the reason why clays are used to interpret the thermal history of a geothermal system, (Reyes, 2000). The results of the XRD analysis of 15 samples selected in the well show the clays to be of three types: smectite, chlorite and illite. The results of the XRD analysis are in Appendix I, while examples are shown in Appendix II. Below is a brief description of the clay types identified.

Smectite is a low-temperature clay alteration mineral occurring as replacement of feldspars, volcanic glass and ferromagnesian minerals and occasionally as vein fillings in voids/vesicles. In XRD analysis, its distinguishing feature is the swelling nature (hence, referred to as swelling clays) of the glycolated sample to a 17-19 Å peak and further reconstruction of the heated sample at 10 Å peak in their first order diffraction. The characteristic peaks notable in this well are at 15.7 Å, 17.3 Å and 10.3 Å for untreated, glycolated and heated samples, respectively. Based on the 15 samples selected for XRD analysis, smectite was only identified at 674-676 m.

Chlorite forms as an alteration product of ferromagnesian minerals, glass or direct deposition in vesicles and veins. Chlorite was observed both in binocular and petrographic analysis and confirmed at selected depths in the XRD analysis. In a thin section, it shows a moderate positive relief with a light green colour, weakly pleochroic and it exhibits first order interference colours from white to yellow. In untreated, glycolated and heated samples, they showed first order peaks ranging from ~14.0 to 14.9Å and a second order characteristic peak at ~7.2-7.3Å that is significantly weakened by the heat treatment of 550°C. Its occurrence in geothermal areas generally indicates temperatures exceeding 220°C (Kristmannsdóttir, 1979). Its first appearance is noted at 604-608 m in XRD and at 510-512 m in a thin section. The occurrence is noted sparingly to 2830 m.

Illite is a type of clay mineral that can be formed as a result of the alteration of potassium and aluminium rich rocks or as an alteration product of other clays. It occurs as a vein and vesicle filling mineral. The

XRD analysis of illite shows no change at the 9.8-10 Å peak in the first order diffraction in the untreated, glycolated and heated samples. In thin sections, it is discerned as colourless to yellow-brown with irregular mottled flakes of crystals and a low refractive index, while in a binocular microscope, it appears metallic brown in colour. In OW-737 illite peaks ranged from 10.2 to 10.3 Å in the first order diffraction. It was first identified at 674 m depth in the XRD analysis and at 402 m depth in a thin section. It is noted to occur sporadically to the bottom of the well. It is indicative of temperatures over 200°C.

4.3 Hydrothermal mineral alteration zones and depositional sequence

Hydrothermal alteration mineral zones in a geothermal system are dependent on temperature, fluid chemical composition and to an extent the depth of occurrence, which relates to pressure. Thus, by mapping alteration minerals, it is possible to establish the alteration mineral assemblages, sequences and zonation. It is also possible to make an outline of the thermal condition and evolution of the geothermal system by examining the order of sequence in which minerals occur and establish if they portray a retrograde or prograde thermal regime.

4.3.1 Hydrothermal alteration zones

Hydrothermal alteration in high-temperature geothermal systems can be divided into a number of alteration zones based on changes in the assemblage of alteration minerals with increasing temperature (Mortensen et al., 2014). The analysis of the drill cuttings revealed five alteration zones, namely unaltered, zeolite-illite, chlorite-illite, epidote-chlorite-illite, and actinolite-epidote-illite zones. The top of each alteration zone is defined by the depth of the first appearance of the index mineral of each zone. In OW-737, they are described as follows.

(i) 0-208 m depth (unaltered zone)
This is the zone from the surface to 208 m depth. The rocks in this zone are relatively unaltered, i.e., they bear no signatures of hydrothermal alteration and the minerals observed are rarely related to hydrothermal fluids of magmatic origin but rather to fluids of meteoric groundwater, that is in contact with the atmosphere. Changes observed are therefore associated with mechanical weathering or variation in atmospheric conditions. Secondary minerals present in this zone are oxides such as limonite and hematite, which are related to the interaction between the rocks and the groundwater. The temperature in this zone is less than 40°C.

(ii) 208-604 m depth (zeolite-illite zone)
Zeolites such as scolecite, mesolite and thomsonite occur in abundance and in association with illite, hematite, limonite and siderite. The zeolitization process reduces the porosity and permeability of the rocks, thereby enhancing the capping mechanisms of this zone. The first appearance of secondary quartz was observed at 490 m depth and therefore the zone indicates a temperature range of 50-180°C. The current water table as measured from reservoir pressure data is at 563 m. This could therefore imply that the water table in the geologic time was more shallow than the present and probably around 300 m depth.

(iii) 604-856 m depth (chlorite-illite)
This zone is characterized by the presence of chlorite that represents a temperature range of 180°C-220°C. Chlorite was observed in this section at 510-512 m, and in XRD strong peaks were seen at 604-608 m. Smectite and zeolites such as scolecite and mesolite are still observable in this zone but they become unstable below 606 m. Other minerals that occur are illite, siderite, calcite, hematite, albite, chalcedony and titanite. Siderite occurrence signifying a low temperature outside this zone could imply it was deposited much later in the system and is therefore not fossil.

(iv) 856-1610 m depth (epidote-chlorite-illite)
The first appearance of epidote is noted at 856 m depth, this indicates temperatures exceeding 230°C (Bird and Spieler, 2004; Kristmannsdóttir, 1979; Reyes, 1990). Other minerals observed include quartz,

calcite, pyrite, wollastonite (first appearance at 1506 m), prehnite and hematite. It is in this zone, where epidote becomes abundant. However, overprinting by calcite is also observed at variable depths, implying an incursion of cooler fluids into the well. The zone indicates a temperature range of 230-270°C before cooling occurred.

(v) 1610-2990 m depth (actinolite-epidote-chlorite-illite)
This zone is marked by the first appearance of actinolite at 1610 m signifying temperatures exceeding 280°C. Other minerals found in this zone include calcite, quartz, wollastonite, titanite, and prehnite. Hematite remains significant to the bottom of the well and there is a notable decline in calcite occurrence and abundance from 2482 m to the bottom of the well.

4.3.2 Hydrothermal alteration minerals paragenetic sequence

Hydrothermal alteration bears signatures that relate to the chemical composition of the fluid and its interaction with rocks, temperature and pressure. It also preserves a paragenetic sequence, which is the order in which the minerals were formed or re-equilibrated and therefore bears a time factor. A paragenetic sequence is established through examining alteration minerals occurring either as depositional in vesicle/void fillings or as the replacement of alteration minerals (e.g. chalcedony>quartz). With the aid of magnifying instruments such as a microscope or hand lens, and depending on the size of the rock sample, one can determine the minerals occurring either as replacement alteration products or as deposition in void spaces. Other features that aid in establishing the paragenetic sequences include cross-cutting relationships, overprinting/overgrowth and textural patterns. In each feature, there are guiding criterions that are used to determine the order of events.

In void space fillings, the paragenetic sequence is determined by using the principle order of mineralization. The mineral that lines the walls of the vein/vugs or fractures formed first and is therefore older than the subsequent layers. Cross-cutting relationships in crystals also help with establishing the paragenetic sequence. In mineral replacement analysis, the replacing mineral product is younger than the replaced primary mineral.

Overprinting features and textural characterization in minerals also provide time diagnostic information on the paragenetic sequence. Where the combination of well-formed crystals (euhedral) and irregularly formed crystals (subhhedral or anhedral) occurs, it is possible that the euhedral was first formed when there was enough space for crystals to fully develop, while subhedral or anhedral crystals were formed later when there was restricted space. A mineral that overprints another is younger than the overprinted mineral. This gives a further indication of the temperature regime that has prevailed. Where a low-temperature forming mineral overprints a high-temperature forming mineral, it implies that there was a shift in the thermal regime and what was originally a hot regime has now become cooler.

During the analysis of hydrothermal alteration minerals in OW-737, the paragenetic sequence of the minerals was investigated to deduce the changes that may have taken place in the reservoir and the relative time scale of their deposition. The representative paragenetic mineral sequences results are presented in Table 5. It presents the three sequences in which the minerals have formed with depth, and they are categorized according to the hydrothermal alteration zones. The mode of occurrence has also been factored in, which shows the minerals to have either formed as depositional in open spaces such as veins/vesicles/fractures or as a replacement of a primary mineral. It is also evident from Table 5 that high-temperature alteration zones are formed dominantly via replacement whereas lower alteration zones are dominantly formed by deposition in veins or vesicles. Table 5 shows that there is a retrograde paragenetic sequence in which lower-temperature minerals are formed at a later phase in the epidote-chlorite-illite and actinolite-epidote-chlorite-illite zones. The sequence demonstrates that the temperature regime in the well has experienced more than one episode of hydrothermal alteration from an initially higher to a low temperature.

TABLE 5: OW-737 alteration minerals paragenetic sequence

Depth (m)	Early ⟶ Later	Mode of occurrence
Sequence 1	*cc> qtz> chl>*	
Zone	*Chlorite-illite*	
674	cc>>qtz	Vesicle
686	cc>>chl	Vein and vesicle
694	cc>>qtz	Vein and vesicle
Sequence 2	*Preh>>epi>>cc> hem*	
Zone	*Epidote-chlorite-illite*	
1152	epi>>qtz	Vesicle/replacement
1172	epi>>cc>>qtz	Vesicle/replacement
1278	epi>>cc>>hem	Replacement
1294	epi>>cc>>hem	Vein/replacement
1418	epi>>cc>>hem	Vesicle/replacement
1422	epi>>cc>>hem	Vesicle/replacement/fracture
1528	epi>>cc	Vesicle/replacement
Sequence 3	*Chl>>Preh>>epi>>wol>>qtz>>cc*	
Zone	*Actinolite-epidote-chlorite-illite*	
1608	epi>>cc	Vesicle/replacement
1646	epi>>qtz	Vesicle/replacement
1756	epi>>wol	Vesicle/replacement
1760	preh>>epi>>cc	Vesicle/replacement
1784	epi>>cc	Vesicle/replacement
2038	Chl>>qtz>>cc	Replacement
2092	epi>>cc	Vesicle/replacement
2150	epi>>cc	Replacement/vein
2476	epi>>cc	Vein/replacement
2538	epi>>cc	Vesicle/replacement
Key: hem=hematite, qtz=quartz, cc=calcite, chl=chlorite, epi=epidote, preh=prehnite, wol=wollastonite		

4.4 Fluid inclusion geothermometry

Fluid inclusion geothermometry, a technique for determining the temperatures at which a crystal formed or recrystallized, involves determining the temperature at which fluid inclusion homogenizes. Fluid inclusion analysis was done on two calcite crystals handpicked at depths between 1410 and 1458 m. The temperature measurement results of 80 fluid inclusions are presented in Figure 8. The homogenization temperature values (T_h) obtained from the two calcite crystals range from 225 to 285°C. Half of the fluid inclusions recorded temperatures between 245 and 265°C, while about 30% represent a homogenization temperature between 225 and 245°C and 20% represent a

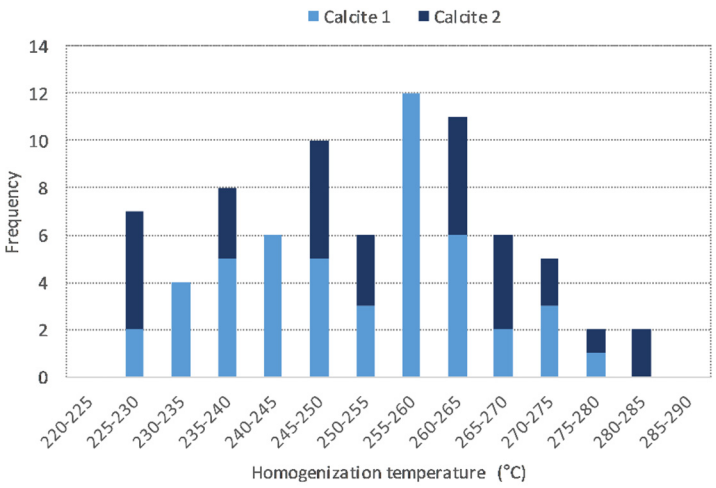

FIGURE 8: OW-737 histogram showing homogenization temperature distribution between 1410 and 1458 m depth from fluid inclusion analysis of calcite crystals

temperature between 265 and 285°C. A distinction between primary, secondary or pseudo secondary fluid inclusions was not made and therefore it is not certain whether the homogenization temperatures represent the thermal regime of the crystal growth or a later regime where fluid inclusions were trapped in imperfections created by fractures.

4.5 Thermal history

To understand the thermal conditions and behaviour of well OW-737 and whether the past conforms to the present, comparisons are made between the formation temperature, alteration mineral temperature and fluid inclusion analysis of homogenization temperature (T_h). A number of studies of temperature dependent alteration minerals, formation temperature and fluid inclusion homogenization temperatures (T_h) have successfully been applied to assess the physico-chemical conditions and the temporal evolution of geothermal reservoirs in active geothermal fields (e.g. Marks et al., 2010). A temperature comparative study may make it possible to decipher the thermal state and history of OW-737, whether it is cooling down, heating up or in equilibrium.

The alteration temperature was obtained from the first appearance of index minerals that are paleo-temperature indicators and they include: quartz (≥180°C), chlorite (≥220°C), epidote (≥230°C), wollastonite (≥270°C) and actinolite (≥280°C). The calculated formation temperature was derived from a Horner plot using the Berghiti program with temperature recovery considered (pre-injection, 9 hrs, 54 days and 99 days). The homogenization temperature was obtained from fluid inclusion analysis that indicates a temperature range from 225 to 285°C. Measured pressure data and boiling point depth data were jointly plotted with results as presented in Figure 9.

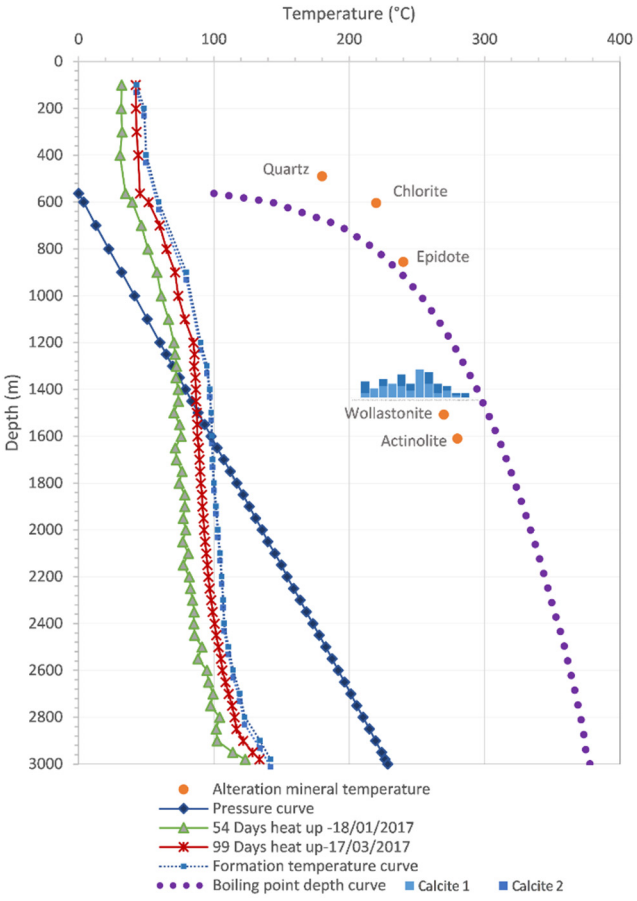

FIGURE 9: OW-737 – plot of pressure, temperatures of heat up, formation temperature, alteration minerals, and boiling depth point

A comparison between the different data sets shows discrepancies and near similarities. A comparison of the calculated formation temperature and alteration temperature from 490 m to the bottom of the well shows the latter to be lower by approximately 140°C. The alteration mineral temperature appears not to differ much with the homogenization temperature. At 1410-1458 m depth, the homogenization temperature ranges between 210 and 285°C, with an average range of 250°C, which fits the epidote temperature range. Within the same depth interval, the formation temperature is 98.3°C, which is much lower than the temperature records of fluid inclusion and alteration minerals. The boiling point depth curve, saturation temperature curve and the calculated formation temperature also appear to differ significantly. In the upper part of the well, the alteration temperature is higher than the boiling point depth curve. This indicates that the present day water table has at some point in the geological time been higher than it is currently. Below 1500 m, the alteration temperature appears to be approximately 30°C lower than the boiling point curve. It is

therefore apparent that significant cooling has occurred in the area since the formation of the high-temperature minerals shown in Figure 9.

4.6 Aquifers and permeability zones

The identification of aquifers/feed zones and permeable zones is done concertedly by incorporating data from geological, drilling and reservoir measurements. Geologically, this is achieved by the examination of rock cuttings, which provides a direct indication of the location of aquifers. Parameters considered include increased alteration intensity, abundance of permeability indicator minerals such as pyrite and platy calcite, presence of vein fillings, indication of fracturing and depths with loss of returns. Geologically, aquifers in OW-737 have been deduced to occur at depths indicated in Table 6, as zones related to increased alteration intensity that coincide with the occurrence and abundance of high-temperature alteration minerals such as epidote, increased oxidation and abundance of vein fillings. The permeable zones also seem to compare well with an increased abundance of calcite, e.g. between 670 and 2164 m and pyrite minerals at 670-2056 m.

Drilling parameters included identifying depths, which experienced increased rates of penetration and loss of circulation during drilling. In this study, data on the loss of circulation during drilling could not be established. Information on ROP, has therefore been used to complement the geological interpretation and this is illustrated in Figure 10. Zones of high ROP at variable intervals between 1220 and 1720 m correspond to areas with increased alteration intensity, e.g. from 1234 to 1620 m. Between 1418 and 1642 m abundance of vein fillings are seen, loss zones at 1668-1692 m and 1514-1540 m, at lithological contacts between trachyte and basaltic intrusion, e.g. at 1278, 1294, 1418 and at 1440 m. High ROP also corresponds to some extent to zones with high abundance of calcites at 1524-1664 m, and pyrite abundance at 1236 m and at 1460-1514 m.

Reservoir techniques for determining permeable zones include pressure response during step rate injection tests, temperature logs during injection and recovery logs during well heat-up and discharge periods. Pressure step rate injection tests provide the injectivity index, which is related to the permeability of the formation. In well OW-737, pressure step rate injection tests were not possible since the well got filled up with water during the injection stages, and hence the injectivity index was not determined. Temperature recovery log measurements are, however, available for the heat up recovery periods (pre-injection, 9 hrs, 54 days and 99 days) as illustrated in Figure 10. These have been used to estimate the feed zones. The feed zones interpreted are small and occur at 1520, 1650, 2150, 2800 and 2850 m depth, which is supported with depths determined from the geology and drilling parameters interpretation.

TABLE 6: OW-737 permeability zones

No.	Depth (m)	Size	Rock type	Remarks
1	490	Small	Rhyolite	Increase oxidation intensity/ fracture related permeability
2	686	Small	Basalt	Veining/vesicles/fracture related permeability
3	950	Small	Trachyte	Loss of returns
4	1200	Small	Trachyte	Fracture/ vein, abundance of calcite and pyrite
5	1418	Small	Trachyte	Increased alteration intensity / fracture/dike intrusion related lithological contact between trachyte and basalt intrusion
6	1526	Small	Trachytic tuff	Increased alteration intensity and calcite related permeability
7	1580	Small	Trachyte	Increased alteration intensity and calcite related permeability
8	1756	Small	Trachytic tuff	Alteration intensity, rock matrix related permeability
9	1840	Small	Brecciated tuff	Fracture/ fault /dike intrusion related permeability. Related to brecciated tuff and basaltic intrusion
10	1892	Small	Trachyte	Increased alteration intensity
11	2032	Small	-	Loss of returns
12	2800	Small	-	Loss of returns
13	2850	Small	Trachyte	intrusion related permeability

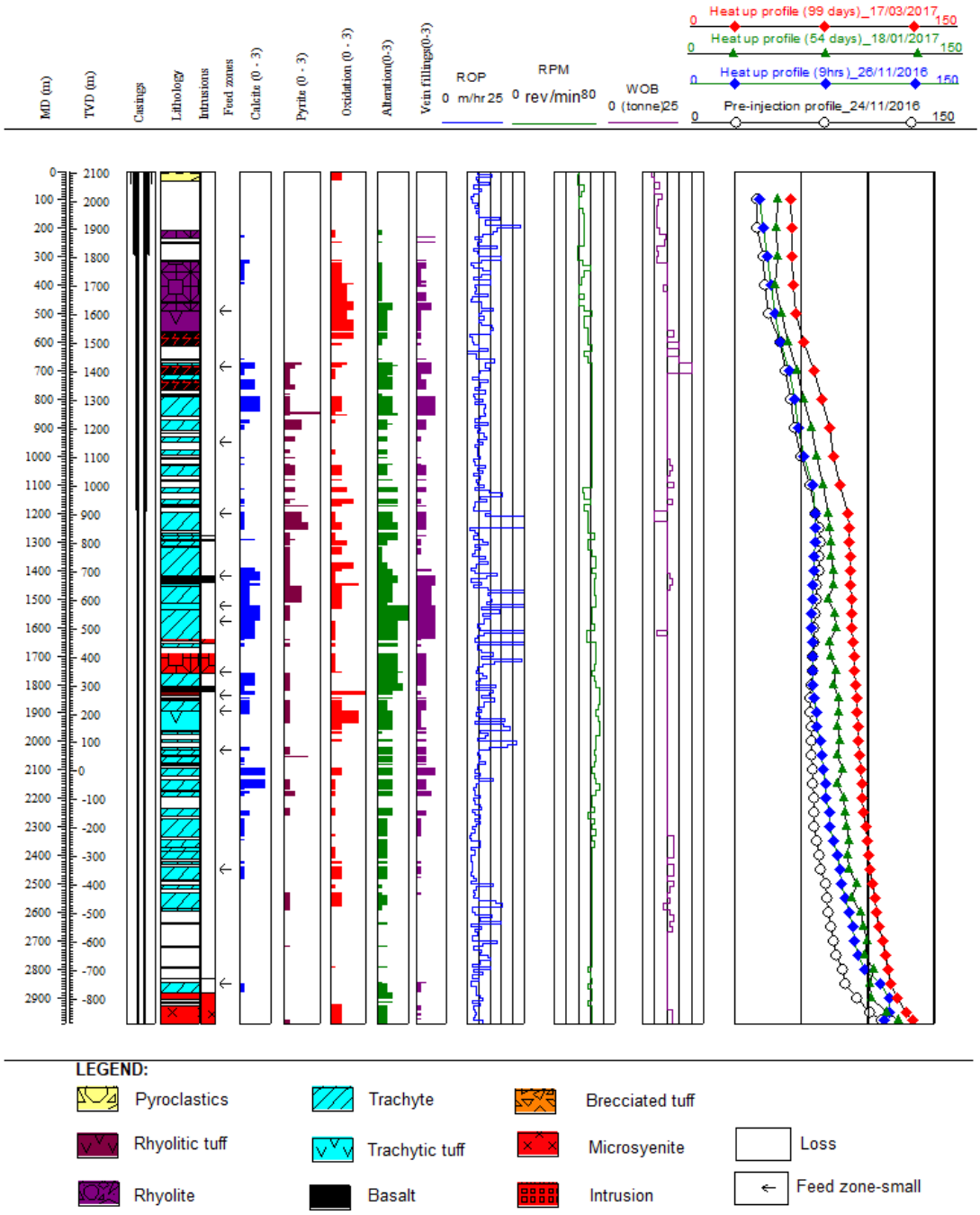

FIGURE 10: OW-737 lithostratigraphy, intrusions, feed zones, alteration minerals, drilling parameters and temperature heat up profiles

It is apparent that the permeability zones deduced in Table 6 have been categorized relatively small to medium on the basis of geological interpretation with contribution from the drilling rate of penetration (ROP). Since the injectivity data, which indicates the current permeability situation, indicates poor permeability in the well, the geological interpretation remains to represent the paleo-permeability of the well.

4.7 Alteration minerals correlation

Comparison of alteration minerals and alteration patterns across wells can provide information on the temperature distribution in a geothermal field and indicate areas of elevated temperature upflows and

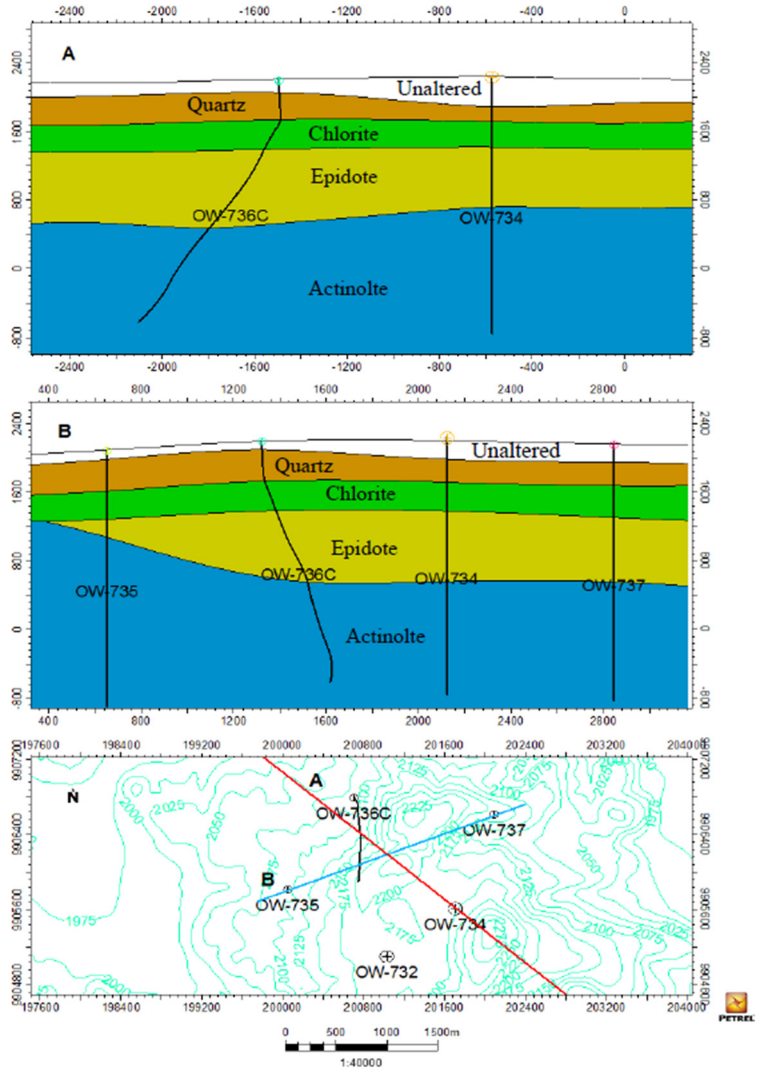

FIGURE 11: Cross-sections showing alteration mineral correlation between wells OW-737, OW-735, OW-734, OW-732 and OW-736C

areas with depressed temperatures as out flows or downflows. To achieve this, the first appearance of selected alteration minerals such as quartz, chlorite, epidote and actinolite that signify paleotemperatures of ≥180, >220, 230 and >280°C, respectively, were considered for wells in the vicinity of OW-737. The wells include OW-736C, OW-735, OW-734 and OW-732. The wells are drilled vertically, except OW-736C. The alteration zones were then modelled in the Petrel platform and two sets of cross-sections selected that run across and along the proximity of OW-737 (Figure 11).

The results as illustrated by cross-section A show the alteration zones of wells OW-736C and OW-734 to be of relatively the same depth and thickness with a slight thinning of the quartz isograd and hence occurring at a relatively elevated depth. Cross-section B shows similarities in the temperature isograds for wells OW-737, OW-736C, OW-734 and OW-732, except for OW-735, where actinolite occurs much shallower. This implies that OW-735 is in a closer proximity to an upflow zone as compared to the other wells. The distribution of calcite and hematite in the correlation wells when jointly plotted with alteration zones could create a better understanding of the indication of cold flow incursions at depth and therefore it should be considered in further investigations.

5. DISCUSSION

Analysis of drill cuttings of Olkaria well OW-737 enabled the characterization of the lithostratigraphy into five lithological series on the basis of mineralogical composition and textural properties. The lithological series are pyroclastics at the top and followed by rhyolites, basalts, trachytes and syenitic intrusions to the bottom of the well. The lithological series are further divided into subseries that have been assigned numbers based on the appearance in the stratigraphic column and on similarities. This was done in an attempt to create a more simplistic way of understanding the lithological sequences and to correlate the lithostratigraphy with wells in the vicinity.

The pyroclastics series is 34 m thick comprising a mixture of eruption materials from Suswa and Longonot. There is a 174 m thick zone of loss of returns between the pyroclastics and the rhyolites. The rhyolites series consists of rhyolites and rhyolitic tuffs with a thickness of 534 m. This zone is also

characterized by significant loss zone. The basalt sequence underlies the rhyolites series and is 214 m thick. It is not uniformly basalt but intercalated with trachytes and rhyolitic tuff. This correlates with the Olkaria basalt in the Olkaria generalized stratigraphic succession (Omenda, 2000), and perceived to be the capping rock formation above the geothermal reservoir.

Below the basalt series is the trachytes series which is the dominant lithology with a 1186 m thickness. The trachytes series has been divided into three major trachyte subseries and in between are tuffs. This sub division is a new categorization of lithological units and is envisaged to be useful for correlation purposes with other wells. This zone is characterized by intrusions of basaltic and rhyolitic composition and thin brecciated and trachytic tuff layers. The lithology is characteristic of the reservoir zone by the presence of high-temperature alteration minerals such as epidote, prehnite, wollastonite and actinolite. The trachyte series compares well with the Plateau trachytes that characterizes the reservoir rocks of the Olkaria geothermal field. The syenite series forms the base below the trachytes series. It is 108 m thick occurring at the bottom of the well. Rhyolitic dike intrusions are likely related to the Olkaria rhyolites that were formed during the last geological event of the Olkaria volcanic history, hence they are probably younger than the basaltic formations. The lithostratigraphic succession of OW-737 therefore conforms to the general lithostratigraphic succession of the Olkaria volcanic complex and as simplified in Table 3, it provides a way of correlation with other wells.

The analysis of alteration minerals in OW-737 shows different minerals categorized by their nature and mode of occurrence as oxides (magnetite, hematite and limonite) calc-silicates (prehnite, zeolites, epidote, titanite, wollastonite and actinolite), clays (smectite, chlorite and illite), secondary feldspars (albite), silica minerals (chalcedony, quartz), carbonates (calcites and siderite) and sulphides (pyrite). It is noted that the degree of alteration intensity increases with depth and the alteration minerals have been formed by processes such as replacement and as deposition in vugs/vesicles, veins or fractures. The alteration minerals signify temperatures which range from low to high.

One of the purposes of the analysis of hydrothermal alteration minerals is to obtain an understanding of the paleotemperature distribution with depth in the well and also to correlate the zones with the wells in the vicinity to decipher if there is a resemblance in the geothermal reservoir parameters, and also whether the upflow or downflow zones which influence the properties of the well are in the proximity of the well. The alteration mineral temperature distribution patterns of OW-737 indicate that the shallow part of the well (less than 500 m) is dominated by low-temperature types of minerals where their formation seems to be controlled by a groundwater system of relatively low temperature. Below 500 m there is a notable increase in alteration with the appearance of greenschist facies minerals such as chlorite and epidote at 512 and 856 m, respectively. Furthermore, the temperature characterization with depth was done by identifying alteration mineral zones based on the first appearance of an index mineral in each zone. Five alteration minerals zones were noted, namely unaltered (0-208 m), zeolite-illite (208-604 m), chlorite-illite (604-856 m), epidote-chlorite-illite (856-1610 m), and actinolite-epidote-illite (1610-2990 m) zones. They represent paleotemperatures of >50, 50-180, 180-220, 230-270 and >280°C, respectively.

The correlation of the alteration zones within wells in the vicinity including wells OW-736C, OW-735, OW-734, and OW-732 has revealed that they are more or less similar and are probably controlled by the same geological conditions. The correlated wells are drilled in close proximity of the studied well. Studies have shown that the Olkaria geothermal system is partly recharged from the North and the Gorge farm fault is one of the significant cold conduits that recharges the geothermal system. This could therefore explain the behaviour of the well as it bears the characteristics of wells drilled in downflow zones. Notable in the well is the occurrence of calcites that seem to prevail in the deeper zones of the well. Many studies have associated calcite presence in geothermal wells to indicate possible boiling conditions and high porosity (Browne, 1984; Omenda, 1998; Muchemi, 1992; Simmons and Christenson, 1994; Okoo, 2014). Where open spaces occur, calcite deposits in response to boiling (Thompson and Thompson, 1996). Simmons and Christenson also mention that calcite forms when there is a mixing of fluids of different compositions. The presence of calcite and hematite near the bottom of

the well could imply that there is incursion of fluids of varying compositions in the well. The determination of the homogenization temperature from fluid inclusion analysis of calcite crystals in this study was only possible at one depth interval, and it indicates some significant cooling has taken place.

The paragenetic sequence investigated in the well shows a sequence of calcite observed to overprint epidote at 1526 m depth. This is believed to imply that the temperature in the well has been declining from an initial high-temperature regime. This signifies the cooling of the reservoir as shown by the mineralogical sequence. This behaviour seems to occur as deep as 2538 m. Hematite, a mineral that indicates the incursion of cooler fluids into the well, has been shown to be common in the well. This seems to support the possibility of the well being situated in a downflow area, where chances are that oxygen rich water is finding its way into the deeper parts of the reservoir.

To further obtain information that explains the temperature situation of well OW-737, other temperature data sets considered included the calculated reservoir temperature, the alteration mineral temperature and fluid inclusion temperature of homogenization (T_h). The results as illustrated in Figure 9 have shown discrepancies between the data sets. The homogenization temperature (T_h) obtained from two calcite crystals at 1410-1458 m are in the range of 225-285°C. When compared with the depth of alteration of selected alteration minerals (Quartz (180°C), chlorite (220°C), epidote (230°C), wollastonite (260°C) and actinolite (<280°C)), it is found that within the same depth range, they seem to compare to some extent but with some indication of cooling. However, an even more exhaustive conclusion could have been obtained if other crystals were available.

It is also discernible from the temperature comparative study that formation temperature calculated from the four heat up recovery periods (pre-injection, 9 hrs, 54 days and 99 days) do not compare with the alteration mineral temperature. It indicates that the present day temperature is less than 100°C and that the alteration minerals represent the fossil state of the geothermal reservoir. The present day water table from the pressure log is at 563 m depth, whereas it appears it was much shallower, at around 300 m depth, when the temperature was the highest according to the alteration minerals temperature curve.

The results from this comparative study can therefore be interpreted to mean that there is a conduit of cold inflow of water into the reservoir, possibly because the well is to the northeast and in close proximity of the Gorge fault, which is a structural feature considered by previous authors to control the recharge to Olkaria geothermal field. This has probably channelled cooler fluids, which have resulted in a cooling down in the well to at least 3 km depth. It can also be observed as the well is trying to heat up gradually, described as isothermal behaviour as displayed in the temperature logs curve. Another explanation could be that the well was considerably cooled during drilling with aerated water, however, there is a lack of circulation loss data to support this. If supported, this could mean that the well is gradually recovering and with time it will stabilize and attain its original condition.

Aquifers in the Olkaria geothermal field can generally be classified as either shallow or deeper. Shallow aquifers are near surface aquifers that are associated with rhyolitic formations. Deeper aquifers are large and intermediate and occur below the cap rock (mostly basaltic) and hosted in trachytic formations. In well OW-737, the occurrence of aquifers has been supported by geological interpretation with zones related to increased alteration intensity that coincide with the occurrence and abundance of high-temperature alteration minerals such as epidote, increased oxidation, abundance of vein fillings, fracturing and intrusions, at lithological contacts and zones of circulation losses. The permeable zones also seem to compare well with the increased abundance of pyrite and calcite minerals. The presence of bladed calcite and calcite with a dogtooth structure were common in the well. Such calcites are interpreted to indicate that there has been high permeability in the geological past, and that this has been compromised in recent times by second generation deposition of e.g. calcites and hematite. Due to a lack of injectivity data that could validate the geologically interpreted permeable zones, the reservoir within the well area can be interpreted to be impermeable in the present day, contrary to the past where the well seemed to be permeable.

6. CONCLUSIONS

The study of well OW-737 with the use of borehole data has provided information on the lithology, temperature, permeability, paragenetic sequences and thermal history. From the interpretation of results and discussion, the following can be concluded:

- The lithostratigraphic succession of OW-737 has been established and categorized into five lithological series, namely pyroclastics, rhyolites, basalts, trachytes and syenitic intrusions series, that are further divided into subseries. Basaltic and rhyolitic dikes are noted to occur as thin intrusions within the trachytic series. The lithostratigraphy to the well bottom (2998 m depth) is found to be in concordance with the general lithostratigraphy of the Olkaria geothermal system, in which the bottom formation is estimated at 6 km depth.
- The OW-737 hydrothermal alteration minerals have been described based on their nature and mode of occurrence as oxides, calc-silicates, clays, carbonates, sulphides, secondary feldspars, and silica.
- Alteration minerals have been found to either form as depositional in open spaces, such as veins/vesicles/fractures, or partly as replacement of primary minerals.
- Five alteration mineral zones defined by the first appearance of index minerals are: unaltered (0-208 m), zeolite-illite (208-604 m), chlorite-illite (604-856 m), epidote-chlorite-illite (856-1610 m) and actinolite-epidote-illite (1610-2990 m). They show that high temperatures have been realized in the past below 1000 m depth as defined by the epidote-chlorite zone marking the top of the geothermal reservoir.
- The paragenetic sequence of the alteration minerals shows that there is a retrograde paragenetic sequence in which lower temperature minerals are formed at a later phase in the epidote-chlorite-illite and actinolite-epidote-chlorite-illite zones. The sequence demonstrates that the temperature regime in the well has declined from initially high temperatures.
- The lack of injectivity shows that presently the well is impermeable. This therefore concludes that the interpreted permeability is fossil and may have decreased due to mineral deposition. This largely remains to be confirmed as the well continues to heat up.
- For the purpose of understanding the thermal evolution of the reservoir confined within OW-737, the calculated formation temperature, alteration mineral temperature and fluid inclusions homogenization temperature (T_h) were compared. The results show a great variation between the formation and alteration temperature suggesting a cooling of the well. The homogenization temperature shows cooling as well to some extent. However, more exhaustive conclusions could have been realized if more fluid inclusions had been analysed at variable depths as well as from other types of minerals, such as quartz. Time did not allow further analysis.
- The present day water table, derived from the pressure log, is at 563 m depth whereas it appears to have been much shallower at around 300 m depth when the temperature was at its maximum, according to the alteration minerals temperature curve.
- An attempt to correlate the OW-737 alteration mineral zones to those of the wells in the vicinity, including OW-736C, 735, OW-734 and OW-732, has shown that they compare well, except OW-735, where the actinolite zone is much shallower suggesting that the well is closer to the upflow zone. In the future, calcite and hematite distribution, if included, will furnish more details about where the cold fluid gets into the reservoir.
- It is evident that this well is drilled outside the upflow zones of the Olkaria geothermal system and most likely it is close or in the downflow zone. Considering that it is drilled outside the Gorge farm fault zone that extends from the ring structure, and that other wells drilled outside (such as OW-922), turned out to be cold, a more comparative study should be undertaken to get a generalized idea about the recharge from the north-northwest trending Gorge farm fault.

ACKNOWLEDGEMENTS

This course would not have been possible without the support of the Government of Iceland and the United Nations University through the Geothermal Training Programme (UNU-GTP) for the award of the fellowship and facilitation and Kenya Electricity Generating Company (KenGen), my employer, for granting approval. My gratitude goes to all of them for their assistance. Special thanks go to the director of the UNU-GTP, Mr. Lúdvík S. Georgsson, deputy director, Mr. Ingimar G. Haraldsson, Ms. Thórhildur Ísberg, Ms. Málfrídur Ómarsdóttir, and Mr. Markús A.G. Wilde for their coordinated assistance to smoothly see me through this course.

I would like to wholeheartedly thank my supervisors Ms. Anette K. Mortensen and Mrs. Helga Margrét Helgadóttir, assisted by Sylvía and Ragna, for their dedicated, tireless guidance and technical support throughout the project. In addition, Mr. Sigurdur Sveinn Jónsson for his assistance in XRD analysis and interpretation, Dr. Hjalti Franzson, Mr. Benedikt Steingrímsson for discussions and to all other ÍSOR staff, who directly or indirectly offered their assistance towards the success of the course. Dr. Gudmundur Ómar Fridleifsson will not be forgotten for enlightening the geological field trip to the Geitafell volcano. Special thanks go to my fellow geologists, Adonias, Andualem, and Tuan Nguyen, for the support we had for each other that really created a homely and conductive environment and to all other 2017 fellows.

Special thanks go to my beloved parents, my family Richard, Mukami, Tetio, Memo and Totti for their endless love, moral support, encouragement and enduring my absence during the six months period.

Finally, I thank the Almighty God for his sufficient grace, love and care that has granted the success of the course.

REFERENCE

Ambusso, W.J., and Ouma, P.A., 1991: Thermodynamic and permeability structure of Olkaria Northeast field: Olkaria fault. *Geothermal Resource Council, Trans., 15*, 237-242.

Baker, B.H., 1987: Outline of the petrology of the Kenya rift alkaline province. *Geological Society, London, Special Publications, 30-1,* 293-311.

Baker, B.H., Mohr, P.A., and Williams, L.A.J., 1972: *Geology of the Eastern Rift System of Africa.* Geol. Soc. of America. Special Paper, 136, 67 pp.

Baker, B.H., and Wohlenberg, J., 1971: Structural evolution of the Kenya Rift Valley. *Nature, 229*, 538-542.

Bird, D.K., and Spieler, A.R., 2004: Epidote in geothermal systems. *Reviews in Mineralogy and Geochemistry, 56*, 235-300.

Bird, D.K., Schiffman, P., Elders, W.A., Williams, A.E., and McDowell, S.D., 1984: Calc-silicate mineralization in active geothermal systems. *Economic Geology, 79*, 671-695.

Bosworth, W., Crevello, P., Winn Jr., R.D. and Steinmetz, J., 1998: Structure, sedimentation and basin dynamics during rifting of the Gulf of Suez and northwestern Red Sea. In: Purser, B.H., and Bosence, D.W.J. (eds.), *Sedimentation and tectonics of rift basins: Red Sea - Gulf of Aden*. Chapman and Hall, London, 77-96.

Browne, P.R.L., 1978: Hydrothermal alteration in active geothermal fields. *Annual Review Earth and Planetary Sciences, 6,* 229-250.

Browne, P.R.L., 1984: Subsurface stratigraphy and hydrothermal alteration of the eastern section of the Olkaria geothermal field, Kenya. *Proceedings of the 6th New Zealand Geothermal Workshop, Geothermal Institute, Auckland, NZ,* 33-41.

Browne, P.R.L., and Ellis, A.J., 1970: The Ohaki-Broadlands hydrothermal area, New Zealand: Mineralogy and related geochemistry. *Am. J. Sci., 269*, 97-131.

Clarke, M.C.G., Woodhall, D.G., Allen, D., and Darling, W.G., 1990: *Geological, volcanological and hydrogeological controls on the occurrence of geothermal activity in the area surrounding Lake Naivasha, Kenya.* Ministry of Energy, Nairobi, Kenya, report, 138 pp. + 3 maps.

Ebinger, C.J., 2005: Continental breakup: the East African perspective. *Astronomy and Geophysics, 46,* 2.16–2.21.

Ebinger, C.J., and Sleep, N.H., 1998: Cenozoic magmatism in Central and East Africa resulting from impact of one large plume. *Nature, 395*, 788–791.

Eshagpour, M., 2003: Borehole geology and alteration mineralogy of well HE-9 in Hellisheidi geothermal field, SW-Iceland. Report 8 in: *Geothermal training in Iceland*. UNU-GTP, Iceland, 165-187.

Gylfadóttir, S.S., Halldórsdóttir, S., Arnaldsson, A., Ármannsson, H., Árnason, K., Axelsson, G., Einarsson, G.M., Franzson, H., Fridriksson, Th., Gudlaugsson, S.Th., Gudmundsson, G., Hersir, G.P., Mortensen, A.K. and Thórdarson, S., 2011: *Revision of the conceptual model of the Greater Olkaria geothermal system - phase I.* Mannvit/ÍSOR/Vatnaskil/Verkís Consortium, report, Reykjavík, 100 pp.

Haukwa, C.B., 1984: *Recent measurements within Olkaria East and West fields.* Kenya Power Co., internal report, 13 pp.

KenGen, 2017: *Geothermal resource map*. KenGen, internal report.

Kristmannsdóttir, H., 1979: Alteration of basaltic rocks by hydrothermal activity at 100-300°C. In: Mortland, M.M., and Farmer, V.C. (eds.), *International Clay Conference 1978*. Elsevier Scientific Publishing Co., Amsterdam, 359-367.

Lagat, J.L., 1998: *Borehole geology of well OW-801, Olkaria Southeast field*. Kenya Electricity Generating Company - KenGen, Kenya, internal report, 12 pp.

Lagat, J.L., 2004: *Geology, hydrothermal alteration and fluid inclusion studies of Olkaria Domes geothermal field, Kenya.* University of Iceland, MSc thesis, UNU-GTP, Iceland, report 2, 71 pp.

Lagat, J.L., 2007: *Borehole geology of OW-904A*. KenGen, Kenya, internal report.

Leach, T.M., and Muchemi, G.G., 1987: Geology and hydrothermal alteration of the North and West exploration wells in the Olkaria geothermal field, Kenya. *Proceedings of the 9th New Zealand Geothermal Workshop, Geothermal Institute, Auckland, NZ,* 187-192.

Mannvit/ÍSOR/Vatnaskil/Verkís Consortium, 2012: *Consultancy services for geothermal optimization study of the Greater Olkaria geothermal fields. Report 8 (revised): proposed field development plan for the Greater Olkaria geothermal field.* Mannvit/ÍSOR/Vatnaskil/Verkís, Reykjavík, report, 98 pp.

Mannvit/ÍSOR/Vatnaskil/Verkís Consortium, 2015: *Provision of consultancy services for undertaking of reservoir model maintenance for the Greater Olkaria geothermal field and training of staff. Report 3: Revision of the numerical model of the Greater Olkaria geothermal system – 2014 phase*. Mannvit/ÍSOR/Vatnaskil/Verkís, Reykjavík, June, 200 pp.

Marks, N., Schiffman, P., Zierenberg, R.A., Franzson, H., and Fridleifsson, G.Ó., 2010: Hydrothermal alteration in the Reykjanes geothermal system: Insights from Iceland deep drilling program well RN-17. *J. Volcanol. & Geothermal Research, 189,* 172-190.

Marshall, A.S.l., Macdonald, R., Rogers, N.W., Fitton, J.G., Tindle, A.G.N., Nejbert, K., and Khinton, R.W., 2009: Fractionation of peralkaline silicic magmas: the Greater Olkaria volcanic complex, Kenya Rift valley. *J. Petrol., 50*, 323-359.

Mechie, J., Keller G.R., Prodehl, C., Khan, M.A., and Gaciri, S.J., 1997. A model for the structure, composition and evolution of the Kenya rift. *Tectonophysics, 278*, 95–119.

Moore, D.M., and Reynolds Jr., R.C., 1989: *X-ray diffraction and identification and analysis of clay minerals* (18th ed.). Oxford University Press, Oxford, 378 pp.

Mortensen, A.K., Egilson, T., Gautason, B., Árnadóttir S., and Gudmundsson A., 2014: Stratigraphy, alteration mineralogy, permeability and temperature conditions of well IDDP-1, Krafla, NE-Iceland. *Geothermics, 49,* 31-41.

Mosley, P.N., 1993: Geological evolution of the late Proterozoic "Mozambique belt" of Kenya. *Tectonophysics, 221*, 223-250.

Muchemi, G.G., 1992: *Geology of the Olkaria Northeast field.* Kenya Power Co. – KPC, Kenya, internal report.

Musonye, X.S., 2015: *Sub-surface petrochemistry, stratigraphy and hydrothermal alteration of the Domes area, Olkaria geothermal field, Kenya*. University of Iceland, MSc thesis, UNU-GTP, Iceland, report 2, 71 pp.

Odongo, M.E.O., 1986: Geology of Olkaria geothermal field. *Geothermics, 15,* 741-748.

Ofwona, C.O., 2002: *A reservoir study of Olkaria East geothermal system, Kenya.* University of Iceland, Reykjavík, MSc thesis, UNU-GTP, Iceland, report 1, 74 pp.

Ofwona, C., Omenda, P., Mariita, N., Wambugu, J., Mwawongo, G., and Kubo, B., 2006: *Surface geothermal exploration of Korosi and Chepchuk prospects*. KenGen, Kenya, internal report, 44 pp.

Okoo, J.A., 2013: Borehole geology and hydrothermal mineralisation of well OW–39A, Olkaria East

geothermal field, Naivasha, Kenya. Report 24 in: *Geothermal training in Iceland 2013*. UNU-GTP, Iceland, 547-574.

Omenda, P.A., 1994: The geological structure of the Olkaria West geothermal field, Kenya. *Proceedings of the 19th Workshop on Geothermal Reservoir Engineering, Stanford University, Stanford, CA,* 125–130.

Omenda, P.A., 1998: The geology and structural controls of the Olkaria geothermal system, Kenya. *Geothermics, 27-1,* 55-74.

Omenda, P.A., 2000: Anatectic origin of comendite in Olkaria geothermal field, Kenya Rift; geothermal evidence of syenitic protholith. *African J. Science & Technology, Science & Engineer. Series*, 1, 39-47.

Otieno, V.O., 2016: *Borehole geology and sub-surface petrochemistry of the Domes area, Olkaria geothermal field, Kenya, in relation to well OW-922.* University of Iceland, Reykjavík, MSc thesis, UNU-GTP, Iceland, Report 2, 84 pp.

Otieno, V.O., and Kubai, R., 2013: Borehole geology and hydrothermal mineralisation of well OW-37A, Olkaria East geothermal field. Report 2 in: *Geothermal training in Kenya*. UNU-GTP, Iceland, 57-105.

Reyes, A.G., 1990: Petrology of Philippine geothermal systems and the application of alteration mineralogy to their assessment. *J. Volc. Geoth. Res., 43,* 279-309.

Reyes, A.G., 2000: *Lectures on petrology and mineral alteration in hydrothermal systems: From diagenesis to volcanic catastrophes.* UNU-GTP, Iceland, report 18-1998, 77 pp.

Ring, U., 2014: The East African Rift System: *Austrian J. Earth Sciences, 107-1,* 132-146.

Roedder, E., 1984: Fluid inclusions. *Mineral. Soc. Am., Rev. Mineral., 12,* 71-77.

Saitet, D., Kamunya, K., Omiti, U., and Okoo, J.A., 2016: *The conceptual model of Olkaria, 2016*. Kenya Electricity Generating Company, Ltd. – KenGen, internal report, 141 pp.

Shackleton, R.M., 1986: Pre-cambrian collision tectonics in Africa. In: Coward, M.P., and Ries, A.C. (eds.), *Collision tectonics.* Geological Society Special Publication*, 19, 329-249.*

Shepherd, T., Rankin, A.H., and Alderton, D.H.M., 1985: *A practical guide to fluid inclusion studies*. Blackie, London, 343 pp.

Simiyu, S.M., and Keller, G.R., 1997: Integrated geophysical analysis of the East African Plateau from gravity anomalies and recent seismic studies. *Tectonophysics, 278,* 291-314.

Simiyu, S.M., and Keller, G.R., 2000: Seismic monitoring of the Olkaria geothermal area, Kenya Rift valley. *J. Volcanol. & Geothermal Research, 95,* 197-208.

Simmons, S.F., and Browne, P.R., 2000: Hydrothermal minerals and precious metals in the Broadlands Ohaaki geothermal system: Implications for understanding low-sulphidation epithermal environments. *Economic Geology, 95-5*, 971-999.

Simmons, S F., and Christenson, B.W., 1994: Origins of calcite in boiling geothermal system. *Am. J. Science, 294,* 361-400.

Smith, M., and Mosley, P., 1993: Crustal heterogeneity and basement influence on the development of the Kenya rift, East Africa. *Tectonics, 12*, 591-606.

SWECO and Virkir, 1976: *Feasibility report for the Olkaria geothermal project*. Report prepared for United Nations and Government of Kenya.

Thompson, A.J.B., and Thompson, J.F.H. (eds.), 1996: *Atlas of alteration: A field and petrographic guide to hydrothermal alteration minerals.* Alpine Press, Ltd., Vancouver, BC, 119 pp.

West-JEC, 2009: *The Olkaria optimization study (phase II) – final reservoir analysis report*. West Japan Engineering Consultants, Inc., 301 pp.

Wheeler, W.H., and Karson, J.A., 1994: Extension and subsidence adjacent to a ‘‘weak’’ continental transform: an example of the Rukwa rift, East Africa. *Geology, 22*, 625-628.

APPENDIX I: XRD results and interpretation

No.	Depth (m)	First order {d(001)} (Å)			Second order{d(002)} (Å)			Alteration mineral
		U	G	H	U	G	H	
1	316-318	-	-	-	-	-	-	none
2	402-404	9.1	9.1	9.1	-	-	-	zeolite?
3	532-534	9.1	9.1	9.1	-	-	-	zeolite?
4	604-606	14.0	14.0	14.0	7.2	7.2	0	unstable chlorite
		8.5	8.5	8.5	-	-	-	amphibole
5	674-676	15.7	17.3	10.3	-	-	-	smectite
		10.3	10.3	10.3	-	-	-	illite
6	716-718	-	-	-	7.3	7.3	0	unstable chlorite traces
7	830-832	14.7	14.7	14.7	7.2	7.2	0	unstable chlorite
8	938-940	14.7	14.7	14.7	7.2	7.2	0	unstable chlorite
9	1004-1008	14.7	14.7	14.7	7.2	7.2	0	unstable chlorite
10	1048-1050	14.7	14.7	14.7	7.2	7.2	0	unstable chlorite
11	1236-1238	10.3	10.3	10.3	-	-	-	illite
12	1328-1332	10.2	10.2	10.2	-	-	-	illite
13	1454-1458	14.9	14.9	14.9	7.3	7.3	0	unstable chlorite
14	1756-1760	14.5	14.5	14.5	7.2	7.2	0	unstable chlorite
		10.3	10.3	10.3	-	-	-	illite
15	2100-2104	14.4	14.4	14.4	7.2	7.2	0	unstable chlorite
		10.3	10.3	10.3	-	-	-	illite
Key: U=untreated, G=glycolated, H=heated								

APPENDIX II: Examples of XRD analyses

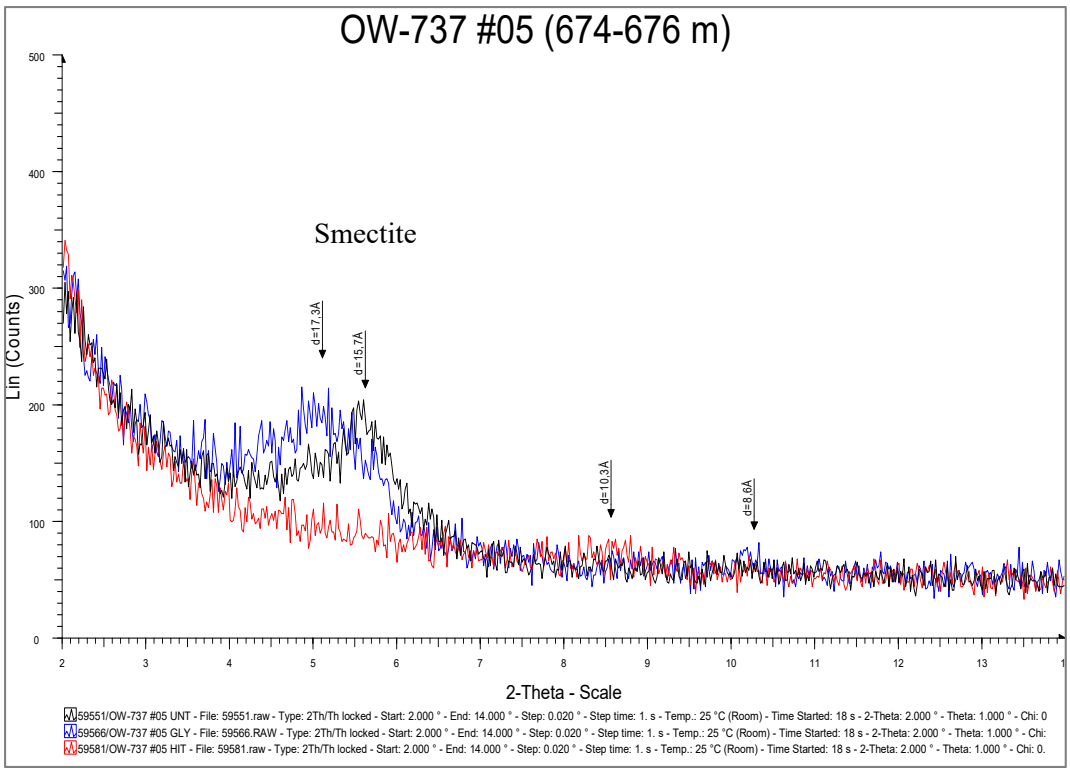

FIGURE 1: XRD analysis showing smectite peaks

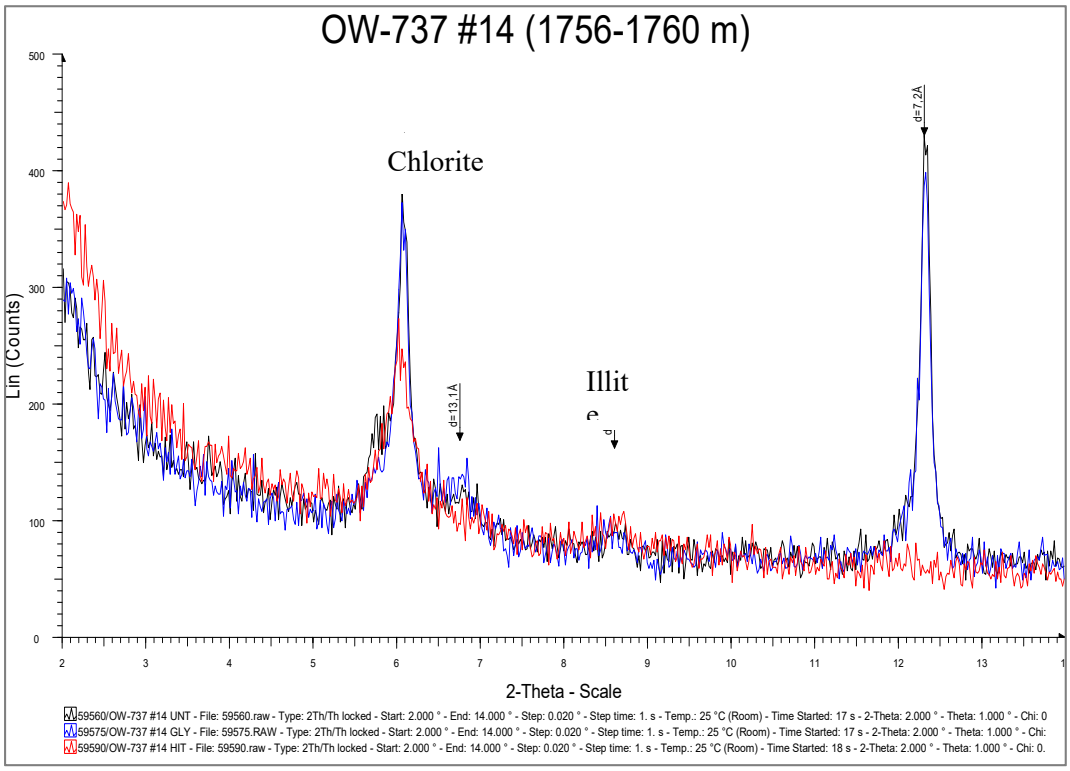

FIGURE 2: XRD analysis showing chlorite and illite peaks